ADVANCED INTELLIGENT SYSTEMS
Open Access
www.advintellsyst.com

Review of Dielectric Elastomer Actuators and Their Applications in Soft Robots

Yaguang Guo, Liwu Liu, Yanju Liu, and Jinsong Leng**

Due to the inherent rigidity of hard materials, the adaptability and flexibility of traditional robots are limited. Recently, soft robots became one of the most attractive areas. The intrinsic compliance and adaptability of soft materials enable soft robots to achieve unexpected functions. Dielectric elastomers (DE) can exhibit large deformation, fast response, and high energy density under the action of external electrical stimuli, becoming one of the most promising materials in soft robots. Herein, the key points of DE actuators (DEAs) are first introduced, including the working principle, DE materials, compliant electrodes, and typical configurations. Then, the soft robots driven by DEAs are reviewed. Some recent highlights are described and discussed in detail. Finally, the main challenges are summarized for the real-world application of soft robots based on DEAs.

1. Introduction

Robots play an increasingly important role in industrial production and daily life. Traditional robots are mostly made of hard materials, such as metal and plastic. Although rigidity of the material enables the traditional robot to perform tasks that are difficult for humans, for instance, carrying heavy objects, it also limits its adaptability. In nature, animals and plants are mostly made of soft materials, which make them have very high compliance and realize a variety of unimaginable actions. Similar to natural creatures, soft robots are usually composed of soft stimuli–responsive materials, which make them have good adaptability and compliance, and can achieve large deformation. Triggered by external stimuli, such as electric fields, magnetic fields, heat, and light, these soft stimuli–responsive materials can deform in a specific direction. The soft stimuli–responsive materials commonly used in soft robots include electroactive polymers (EAP),[1–3] hydrogels,[4–7] magnetic materials,[8–10] shape memory polymers (SMP),[11–13] shape memory alloys (SMA),[14,15] liquid crystal elastomers (LCE),[16–18] and so on. In addition, other actuation methods, such as pneumatic inflation and[19] electrostatic,[20,21] are also widely used in soft robots. To have an overview of different actuation methods, their performances with the maximum values are shown in **Table 1**. Although these maximum values were obtained from different actuators for each actuation method, they still demonstrate the potential upper limit.

Dielectric elastomer (DE) is a typical EAP, which can generate significant deformation under the action of an external electric field. Thanks to its characteristics, such as large deformation,[22,23] fast response,[24,25] low elastic modulus,[2] high energy density,[26,27] light weight,[28,29] and low cost,[28] DE has the reputation of artificial muscles and has become one of the most promising materials in soft robots.[30–34]

In this Review, we concentrate on the recent progresses of dielectric elastomer actuators (DEAs) and their application in soft robots. In Section 2, we first introduce the working principle of DEAs, followed by the DE materials and compliant electrodes. Then, various DEAs with different designs are introduced. In Section 3, the application of DEAs in soft robots is divided into seven categories. Some recent highlights are described and discussed in detail, especially those with biological inspiration. We summarize some of the challenges in Section 4 and this is followed with the conclusion in Section 5.

2. Dielectric Elastomer Actuators

2.1. Working Principle

Generally, the structure of a DEA is similar to a sandwich, consisting of a DE membrane, where both surfaces are coated with compliant electrodes, as shown in **Figure 1**a. Once the compliant electrodes are subjected to voltage, an electric field will be generated in the membrane. The induced Maxwell stress causes the membrane to expand its area and contract its thickness. Based on the mechanism of converting electric energy into mechanical

Y. Guo, Prof. L. Liu, Prof. Y. Liu
Department of Astronautical Science and Mechanics
Harbin Institute of Technology (HIT)
P.O. Box 301, No. 92 West Dazhi Street, Harbin 150001, China
E-mail: liulw@hit.edu.cn

Prof. J. Leng
Center for Composite Materials and Structures
Science Park of Harbin Institute of Technology (HIT)
P.O. Box 3011, No. 2 YiKuang Street, Harbin 150080, China
E-mail: lengjs@hit.edu.cn

The ORCID identification number(s) for the author(s) of this article can be found under https://doi.org/10.1002/aisy.202000282.

DOI: 10.1002/aisy.202000282

Table 1. Comparison of different actuation methods.

Actuators	Strain [%]	Stress [MPa]	Relative speed	Work density [kJ m^{-3}]	Efficiency [%]	References
SMAs	10	200	Slow	10^5	10	[33,191]
SMPs	400	4	Slow	2000	10	[30,192]
Ionic gels	40	0.3	Slow	60	30	[30]
DEAs	503	7.7	Fast	3400	90	[30,33,58,193]
Ionic polymer metal composite	40	3	Slow	5.5	1.5	[33]
Piezoelectric ceramic	0.2	110	Fast	100	90	[30,192]
Pneumatic actuators	50	1.16	Medium	500	49	[33,191,194,195]
Hydraulically amplified self-healing electrostatic actuators	170	0.3	Medium	64.4	21	[33]
Natural muscle	40	0.35	Medium	40	40	[30,33]

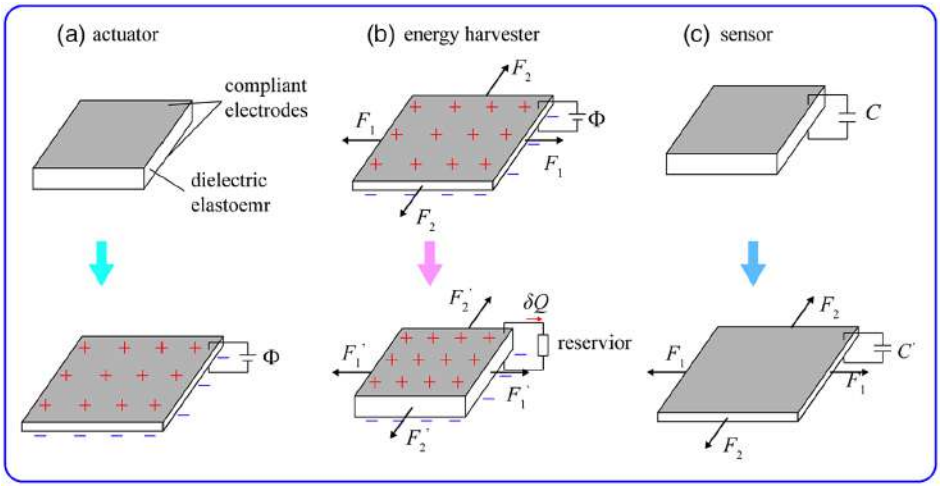

Figure 1. Working principle.

energy directly, the DE has been designed into various configuration actuators, soft robots, etc.[31,32] In contrast, DEs can also be used as energy harvesters to convert mechanical energy into electrical energy.[35–37] On the contrary, the structure of DEA is similar to the capacitor, and the deformation will lead to change in the capacitance value, so it can also be used as a flexible sensor.[38,39]

2.2. DE Materials

As the most important component of DEAs, the properties of DE materials have a crucial impact on the performance of DEAs. To obtain better performance, the material is required to have low modulus, low viscosity, high electrical breakdown strength, and high dielectric constant.[40] In the past research, various materials have been investigated experimentally, and the commonly used materials can be divided into three categories: acrylics, silicones, and polyurethanes (PUs). Acrylic elastomers (VHB 4910 and VHB 4905, 3M Company) are the most used materials in experiments because they are commercially available and inexpensive. It can produce larger voltage-induced strain, such as linear strain over 380%[1] and area strain over 2200%.[22] However, the viscoelastic nonlinearities in acrylic elastomers seriously affect the performance of DEAs, especially the response time.[41,42] Silicone elastomers exhibit modest actuation strain compared with acrylic elastomers. Due to the lower dielectric constant, it requires a higher voltage to achieve larger strain. However, the much lower viscoelasticity allows silicone-based DEAs to operate at high frequencies.[30,43] PUs can generally provide larger output force. A lower electric field can drive DEAs based on PUs due to its inherent higher dielectric constant. However, the higher modulus results in relatively small strain.

2.3. Compliant Electrodes

As another important component of DEAs, compliant electrodes also affect the functionality of DEAs to a great extent. The electrodes generally should have the properties of high compliance, high conductivity, good stability, and strong adhesion to the membrane. The most commonly used compliant electrodes in DEAs include carbon grease, carbon powder, carbon nanotubes

(CNTs), and graphite.[30,44–48] Among these available choices, carbon grease is the most widely used because it is cheap, highly compliant, and easily accessible. However, the drawback of carbon grease is that the oil in carbon grease will dry after a long time. Carbon powder and graphite are more suitable for multilayer stacked DEAs because they are easy to apply on the surface of the membrane and they are very thin. However, the conductivity will be reduced due to the loss of contact between the powders under a higher strain. CNTs and silver nanowires (AgNWs) have also been used as compliant electrodes in the design of adaptive optical devices due to their high conductivity and highly transparent.[49–51] Ionic conductors are also promising candidates as compliant electrodes in the application, such as camouflage, optical devices, etc., due to the advantages of optical transparency and self-healing.[52–57]

2.4. Configurations of Typical DEAs

In the field of DE, one of the main goals is to develop high-performance DEAs. Based on the working principle, various configurations of DEAs are designed for extensive applications, such as planar,[58–66] multilayer stacked,[26,27,67–71] folded,[72,73] rolled,[24,74–78] diamond,[79–81] bending,[82–86] zipping,[87] balloon,[22,23,88–93] cone-shaped,[94–101] hinge,[102–105] rotary,[106–110] and so on, as shown in **Figure 2**. The actuation performance of some existing DEAs is shown in **Table 2**.

As shown in Figure 2a, the simplest structure of DEA is a membrane coated with compliant electrodes on both surfaces. Many kinds of DEAs use this kind of plane deformation to achieve linear displacement. For example, Plante et al.[79] presented a diamond DEA. The prestretched DE membrane was sandwiched between a pair of diamond-shaped structural frames. The area expansion of the DE membrane is transformed into a linear displacement of the diamond DEA. In contrast, the deformation in the thickness direction of the DE membrane can also be used. However, the deformation in the thickness direction of the single-layer membrane is too small to be utilized. Therefore, a multilayer stacked DEA is developed to increase the deformation in the thickness direction. Kovacs et al.[27,67] presented a multilayer stacked DEA using the stress-free interpenetrating polymer network-modified acrylic membrane to replace the prestretched acrylic membrane. The actuator weighs about 4 g and is able to lift a weight of over 2 kg. However, the fabrication would become more difficult as the number of layers gradually increases, especially, the DEA is fabricated by hand in the early stage. To solve this problem, Maas et al.[71] presented a novel automated process to manufacture a multilayer stacked DEA. This technology makes DEA possess homogeneous and reproducible properties. Alternatively, folded DEA is proposed with a simpler fabrication procedure.[72] In addition, Zhao et al.[111] proposed a compact DEA by rolling a long multilayer stacked DE sheet. It converts the biaxial expansion into linear movement along the axial direction, while increasing the output force. Within a volume less than 1 cm^3, the actuator can produce 1 N blocked force and 1 mm free displacement.

The prestretch has a significant impact on the performance of DEA. For instance, it can suppress electromechanical instability and increase actuation strain.[112] Huang et al.[75] introduced a rolled DEA made of fiber-stiffened elastomer sheets. The actuator can achieve strain of 28.6% without prestretch and the strain increased to 35.8% with a prestretch of 40%. Moreover, Pei et al.[76,113] added a compressed spring inside the rolled DEA to maintain the axial prestretch of the membrane. The spring rolls with 2-degree-of freedom (DOF) and 3-DOF are capable of bending as well as axial linear actuation by patterning two or four circumferential electrodes.

When a DE membrane is mounted on a chamber of air, the membrane will be inflated into a balloon. Under the coupling effect of voltage and internal pressure, the DE balloon would experience electromechanical instability or snap-through instability easily. A giant voltage-induced area strain of 1692% is achieved with suitable parameters.[23] Due to this large deformation, the DE balloon is also used for large-volume fluid pump[93] and trigger actuator.[92]

The cone actuator is named by its shape in which the DE membrane is fixed on a rigid frame and subjected to bias force perpendicular to its plane. When the membrane is subjected to a voltage, it expands and tension within it is reduced, and the displacement occurs in the direction of bias force. Rossiter et al.[94] present an antagonistic structure of cone DEAs. The two circular membranes are 3D printed and prestretched by the rigid rod in the center. To maintain the deformation of DEA without continuously applying voltage, Wang et al.[101] introduced a bistable structure in a double-conical DEA. The buckling beam allows DEA to switch not only between the two stable states of translation, but also between the two stable states of rotation. On the other side, Hau et al.[96] demonstrated a high output force and stroke DEA by combining stacked DE films. The prototype shows outstanding performance with an output force of 100 N and a stroke of 3 mm. Inspired by biological agonist–antagonist systems, Lochmatter et al.[102] proposed a DEA in the form of an active hinge. It consists of a hinge support structure and prestretched DE membrane attached to both sides. When the membrane on the onside is subjected to a voltage, the stress within it is reduced and the structure rotates to the opposite side.

Compared with traditional mechanical devices, the advantages of soft actuators or soft robots are softness and large deformation. However, the rigid frame introduced to keep the film prestretched is not conducive to the development of soft robots. Kofod et al.[82] proposed self-organized DE minimum-energy structures (DEMES). The prestretched DE membrane is attached to a thin plastic frame and it will self-organize into a complex structure with minimal energy when it is released from the prestretch frame because the frame made of plastic such as polyethylene terephthalate (PET) is flexible but not stretchable. When the DE membrane is subjected to voltage, the stress inside the membrane is redistributed, and the structure tends to be flat.

In addition to the actuation function, DEAs can also sense the change in capacitance during deformation, as described in Section 2.1. Therefore, some DEAs with self-sensing capability have been developed.[114–117] For instance, Landgraf et al.[117] presented a new method of superposition of driving and sensing signals to realize the self-sensing function of DEAs. It has been validated experimentally and is a promising approach to miniaturize circuits.

Table 2. Summary of typical DEA actuation indexes.

Types of DEAs	Actuation index			Reference
Planar actuator	Linear strain 503%			[58]
	Linear strain 360%			[59]
	Linear strain 230%			[60]
	Linear strain 142%			[152]
	Linear strain 90.6%			[63]
	Linear strain 50%			[196]
	Linear strain ≈50%			[65]
	Linear strain 38%			[184]
	Linear strain 12%			[61]
	Areal strain 488%			[66]
	Areal strain 230%			[197]
Multilayer stacked/folded actuator	Linear strain 46%	Lift a weight of over 2 kg	Energy density 12.9 J kg^{-1}; ≈500 cycles	[27,67]
	Linear strain 24%	Linear pull force ≈70 N	Energy density 19.8 J kg^{-1}; ≈300 000 cycles	[26]
	Linear strain ≈15.5%			[72]
	Linear strain ≈10%	Raise a load of 900 g		[68]
	Linear strain ≈4.6%		Nature frequency ≈31 Hz	[69]
	Linear strain 3.5%	Tensile force 10 N		[71]
Rolled actuator	Linear strain ≈200%			[77]
	Linear strain ≈70%			[78]
	Linear strain 35.8%			[75]
	Linear strain 25%	Blocked force 0.44 N	Power density 1.2 kW kg^{-1}	[139]
	Linear strain 15%			[157]
	Linear strain 15%		Energy density: 1.13 J kg^{-1}; bandwidth >400 Hz; ≈600 000 cycles	[24]
	Linear strain 9.75%	Blocked force 1 N	Energy density 0.275 J kg^{-1}; ≈50 000 cycles	[111]
	Bending angle 90°	Lateral force 0.7 N; blocked axial force 15 N		[76]
Minimum energy structures	Angle change 0°–90°			[82]
	Angle change ≈−70°–80°			[84]
	Displacement change −40–35 mm		Per action 0.1386 J	[119]
	Angle change 82.4°	Blocked force 143 mN		[86]
	Angle change 0°–52.8°			[198]
Balloon actuator	Areal strain 2200%		Electromechanical energy conversion density 1.13 J g^{-1}	[22]
	Areal strain 1692%			[23]
	Areal strain 1165%			[199]
	Areal strain 400%	Force 0.15 N		[200]
	The apical displacement 6.3 mm			[201]
Cone-shaped actuator	Linear displacement 7.1 mm		Power density 108.9 W kg^{-1}	[202]
	Linear displacement ≈4.5 mm			[203]
	Linear displacement 4.06 mm			[97]
	Linear displacement 3 mm	Force 100 N	1.62 J cm^{-3}	[96]
	Linear displacement ±0.16 mm	Blocked force ≈0.31 N		[94]
	Rotation angle 9.6°			[99]

Table 2. Continued.

Types of DEAs		Actuation index		Reference
Others	Linear displacement ≈8 mm			[204]
	Linear displacement 300 μm			[87]
	Rotation angle ≈7.5°			[109]
	Speed 19 rpm	Torque 0.031 mNm		[108]
	Speed 1500 rpm		Accumulated several tens of millions of cycles	[107]
		Blocked torque 18 mNm	Specific power 20.8 W kg^{-1}	[106]
	Rotation angle ≈24°	Blocking force ≈0.5 N		[102]

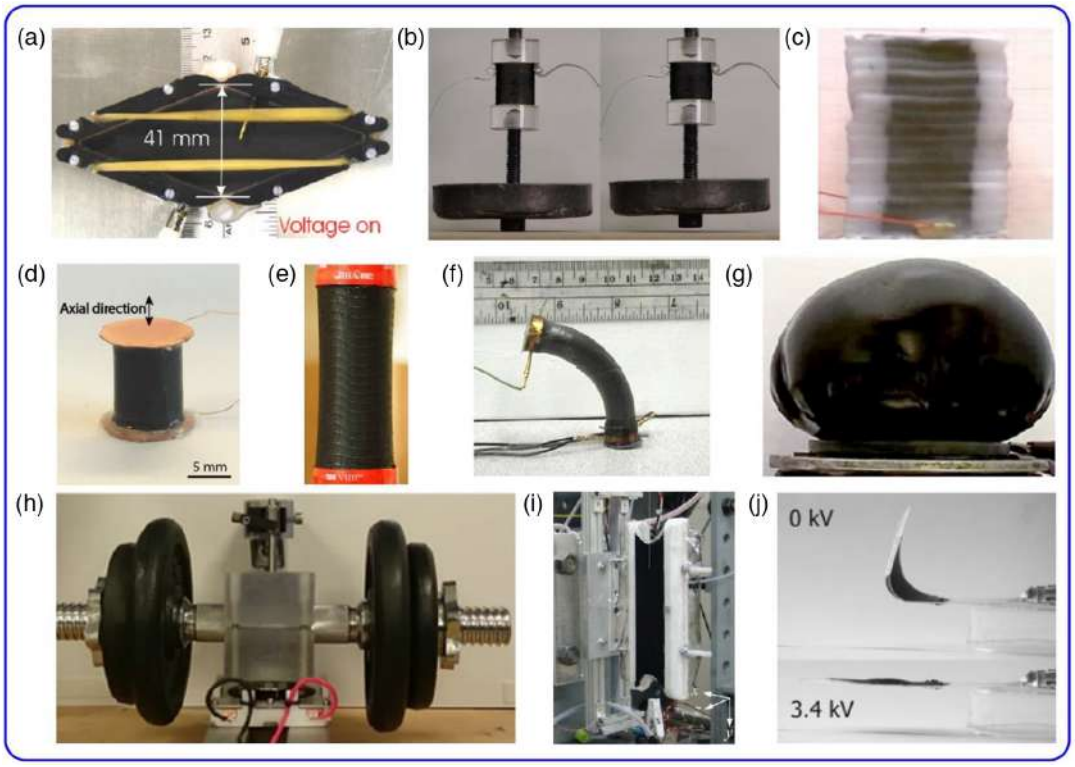

Figure 2. Configurations of typical DEA. a) Diamond DEA. Reproduced with permission.[79] Copyright 2007, Elsevier. b) Multi-layer stacked DEA. Reproduced with permission.[27] Copyright 2009, Elsevier. c) Folded DEA. Reproduced with permission.[72] Copyright 2007, IOP Publishing. d) Compact DEA. Reproduced with permission.[111] Copyright 2018, John Wiley and Sons. e) Rolled DEA. Reproduced with permission.[75] Copyright 2012, AIP Publishing. f) Spring rolls. Reproduced with permission.[76] Copyright 2004, IOP Publishing. g) A DE balloon. Reproduced with permission.[23] Copyright 2013, Elsevier. h) High force cone DEA. Reproduced with permission.[96] Copyright 2018, Elsevier. i) Active DEA hinge. Reproduced with permission.[102] Copyright 2008, Elsevier. j) Minimum-energy structures. Reproduced with permission.[82] Copyright 2006, Springer Nature.

3. Application in Soft Robots

In recent years, soft robots have attracted more interest from researchers due to their compliance and flexibility. The distinctive performances of DEAs provide more opportunities for soft robots. For example, the simple actuation mechanism makes it easier to design more structures of soft robots. It also provides new options for mimicking different natural creatures, which makes the soft robots have better adaptability in uncertain environments. Based on the various configurations of DEAs, researchers have designed and developed a variety of soft robots. The following subsections review DEAs in the application of soft grippers, walking/crawling robots, jumping/flying robots, swimming robots, humanoid robots, tunable lens, and tactile displays.

3.1. Soft Grippers

In the field of soft robots, grasping objects of different shapes and types is one of the most challenging problems. DEA provides a solution to this issue due to its inherent flexibility, and various configurations of soft grippers based on DEAs have been developed, as shown in **Figure 3**. DEMES can self-organize from a flat state into a complex out-of-plane structure, with light weight and large deformation. Kofod et al.[118] developed a tulip-shaped soft

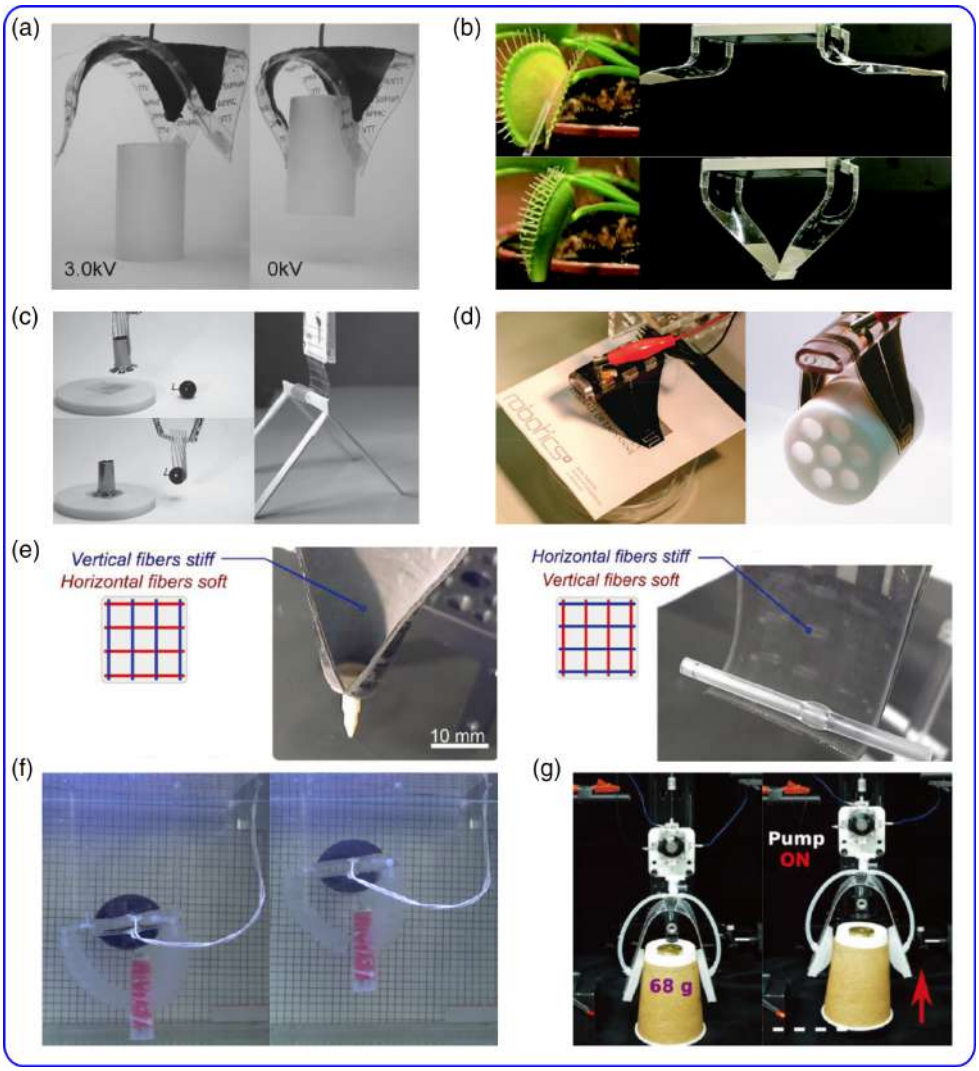

Figure 3. Soft grippers. a) Tulip-shaped soft gripper. Reproduced with permission.[118] Copyright 2007, AIP Publishing. b) Bistable soft gripper. Reproduced with permission.[119] Copyright 2018, Springer Nature. c) A soft gripper constrained by stiff fibers. Reproduced with permission.[2] Copyright 2015, John Wiley and Sons. d) Soft gripper coupling with electroadhesion. Reproduced with permission.[120] Copyright 2015, John Wiley and Sons. e) Reconfigurable soft gripper. Reproduced with permission.[122] Copyright 2020, John Wiley and Sons. f) Hydraulic soft gripper driven by DE balloon. Reproduced with permission.[123] Copyright 2018, IOP Publishing. g) Pneumatic soft gripper driven by DE pump. Reproduced with permission.[25] Copyright 2019, John Wiley and Sons.

gripper based on DEMES, as shown in Figure 3a. When the actuator is subjected to voltage, the gripper opens to envelop the object. When the voltage is turned off, the gripper contracts, and the three claws hold the object to manipulation. To expand the applicability of DEMES gripper, Araromi et al.[29] presented a new design of DEMES with multisegments. The repetitive segments enable the gripper to grab objects of different sizes and shapes. DEMES generally operate in a push–pull configuration, which means that maintaining the open configuration requires continuous energy consumption. Inspired by Venus flytrap, Wang et al.[119] designed a soft gripper based on bistable DEMES. The gripper consists of a PET frame mounted by two prestretched DE membranes on both sides. When an impulse voltage is applied, the gripper can quickly switch (0.17 s) between two stable states, thus grasping or releasing the object. Therefore, the energy consumption per grasping action can be as low as 0.1386 J. Alternatively, Shian et al.[2] incorporated stiff fibers into DEA to induce the deformation of the soft gripper. By adjusting the arrangement of the stiff fiber, the soft gripper can produce wrapping or bending action to stimulate gripping objects of different shapes.

Various methods have been adopted to reinforce the grasping capability of soft grippers. For example, Shintake et al.[120] introduced a soft gripper with electroadhesion. When voltage is applied to DEA, the gripper is closed to grip the object. Then voltage is applied to the electrode pattern of electroadhesion, and an attractive force is generated between the target object and the gripper to enhance the grasping force. In addition, the researchers also combined variable-stiffness materials with DEA-based grippers to enhance its performance. Shintake et al.[121]

designed a soft gripper with variable stiffness. The gripper is composed of a DEA that generates a bending actuation and silicone substrate embedded with low-melting-point alloy (LMPA). The controllable stiffness is achieved by the phase change of LMPA through joule heating. When LMPA is in the solid state, the gripper can maintain its shape and obtain high holding force due to high stiffness. When LMPA becomes liquid by joule heating, gripper can change its configuration under the action of voltage. Aksoy et al.[122] proposed a reconfigurable soft gripper combining a DEA with two layers of SMP fibers and an array of stretchable heaters. Selective joule heating can change the local stiffness of the SMP fibers, and DEA can bend along a soft axis, enabling the gripper to morph into multiple configurations, as shown in Figure 3e. This property of variable stiffness will further expand the applicability of the soft gripper.

In addition to the aforementioned soft grippers made directly from DEAs, researchers also combine other technologies to make DEA-driven soft grippers. Pneumatic actuator is also widely used in the design of soft robots, thanks to its large deformation and high output force. However, the heavy rigid hydraulic source limits its compliance. Inspired by the bladders and hydrostatic skeleton, Zhang et al.[123] proposed a soft hydraulic gripper. A DE balloon was used as the soft hydraulic source instead of the traditional rigid pump to drive the hydraulic gripper made of hydrogel. Moreover, Cao et al.[25] presented a pneumatic pump driven by a magnetically coupled DEA (MCDEA). It can reach maximum output pressure of 30.5 mbar and a flowrate of 0.9 L min^{-1} at resonance. The MCDEA pump was successfully integrated into a soft gripper and grasped an object weighing 68 g. This combination of the two technologies will provide more opportunities for soft robots.

3.2. Walking/Crawling Robots

In the early works of DEAs in the application of soft robots, Eckerle et al.[124] developed the first biomimetic walking robot driven by DEA, named FLEX. It has six legs, and each leg has two degrees of freedom. However, the walking speed is too slow. Later, an improved FLEX2 was developed by the same group, and the walking speed reached 3.5 cm s^{-1}.[125] Although the performance of DEA-driven Flex and Flex2 is not good, it is still a huge progress in the development of DEA, which proves that DEA can be used in robots. Further, Pei et al.[76,126] developed two kinds of six-legged robots based on the spring roll actuator. Skitter was built with six single-degree-freedom spring roll actuators, and a peak speed of close to 7 cm s^{-1} was achieved. As shown in **Figure 4**a, MERobot was designed with six 2-DOF spring roll actuators as legs. The maximum walking speed of 13.6 cm s^{-1} is achieved at 7 Hz. In

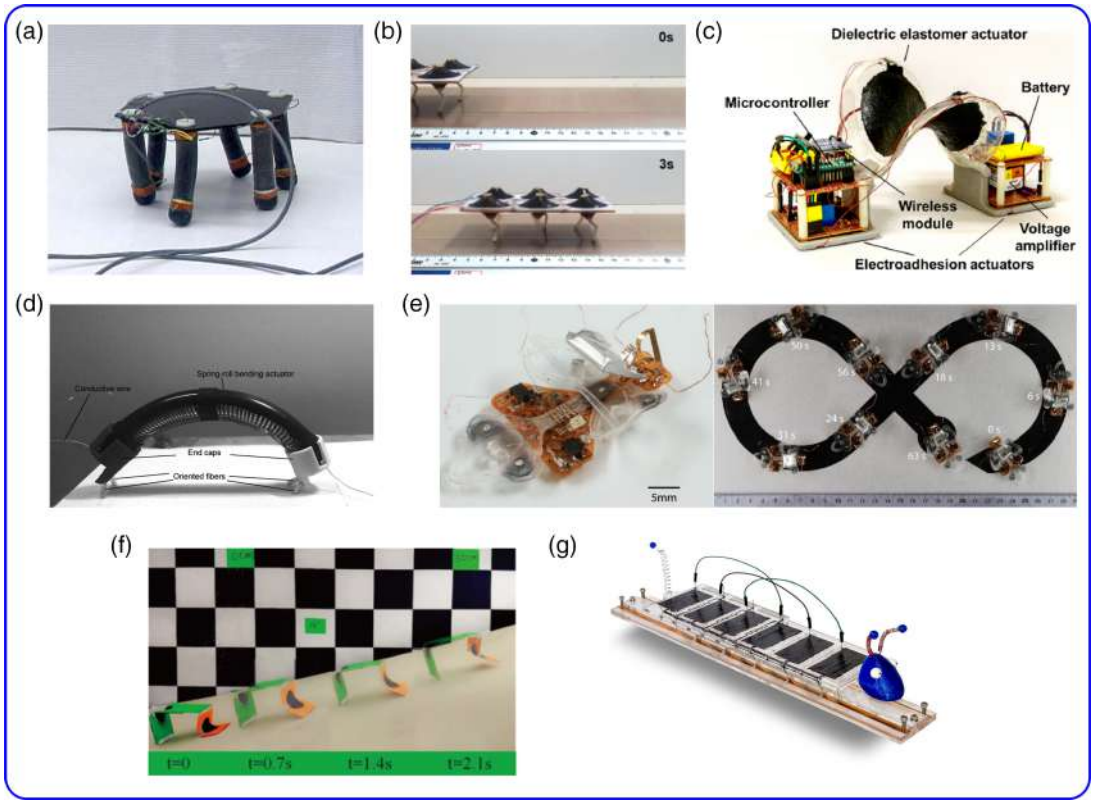

Figure 4. Walking/crawling robots a) MERbot. Reproduced with permission.[76] Copyright 2004, IOP Publishing. b) Hexapod walking robot. Reproduced with permission.[127] Copyright 2017, Elsevier. c) Untethered soft robot. Reproduced with permission.[128] Copyright 2018, Elsevier. d) Soft crawling robot. Reproduced with permission.[74] Copyright 2019, Mary Ann Liebert, Inc. e) Untethered soft robotic insect. Reproduced with permission.[131] Copyright 2019, The American Association for the Advancement of Science. f) Hopping–running robot. Reproduced with permission.[132] Copyright 2019, The American Association for the Advancement of Science. g) A robot with integrated artificial nervous system. Reproduced with permission.[134] Copyright 2018, IOP Publishing.

recent works, Nguyen et al.[127] presented a hexapod walking robot driven by another kind of multi-degree-of-freedom DEA. The cone DEA of antagonistic configuration can generate 3-DOF by dividing the electrode into four independent regions. By imitating the animal's walking posture, the walking robot can achieve an average speed of 3 cm s^{-1}. Unlike these legged robots, researchers have also developed a variety of crawling robots inspired by natural creatures. Inspired by inchworms, Cao et al.[128] introduced an untethered soft robot that consists of a DEMES body and two electroadhesion feet. With the strong electroadhesion, the robot can move forward or backward stably under the action of electronic components integrated into the feet. Similarly, Gu et al.[129] developed a tethered soft robot that can climb various walls. Based on the spring roll bending actuator, Li et al.[74] developed a soft crawling robot. At each end of the actuator, there are two bundles of oriented plastic fibers to provide fraction. At a frequency of 20 Hz, the robot can reach a speed of 26.3 mm s^{-1}. In nature, insects are remarkably agile and robust. Researchers are also working on insect-scale soft robots. For example, Li et al.[130] developed an insect-scale soft robot. Because of its soft body made of silicone, it can survive the pressure of 30 000 times its weight. Generally, the voltage for driving DEAS is as high as several kilovolts. How to make a DEA-based soft robot driven by a voltage of less than 1000 V has always been a concern of researchers. Ji et al.[131] introduced a low-voltage-stacked DEA with a working voltage of less than 450 V and used it to propel an untethered soft robotic insect with a length of about 40 mm. The moving speed of the robot under no load is up to 30 mm s^{-1}. Zhao et al.[132] proposed a hopping–running robot with high speed based on the DEMES. Inspired by rabbit, two DEMES joints were used as the foreleg and hind leg, respectively. With lightweight of 6.5 g, the robot can reach a speed of 51.83 cm s^{-1} (6.10 body lengths/second). Different from these soft robots controlled by traditional hard electronic components, Henke et al.[133,134] designed a soft robot with an integrated artificial nervous system. By providing external DC voltage, the deformation of DEA will change the state of DE switch and vice versa. The alternating in-plane deformation of multiple DEAs is transformed into a caterpillar-like crawling motion. This work highlights that the soft robot with this kind of artificial nervous system can automatically generate all the signals for the requirement of DEAs. The performance and characteristics of walking/crawling robots are summarized in **Table 3**.

3.3. Jumping/Flying Robots

Jumping is a common locomotion type in nature because it is fast and efficient. In the early works, Pei et al.[135] developed a hopping robot using DEA. The hopping robot is very simple and lightweight. Three DEAs in flat configuration were used to actuate the three legs of the hopping robot, respectively. The size of the hopping robot is ≈5.5 cm × 5.5 cm × 1.5 cm. When voltage is applied, DEAs achieve out-of-plane motion, causing the robot to jump. It can jump ≈2 cm (1.33 times its body height). Inspired by click-beetles and simple biomechanical models, Dudutat et al.[136] designed a jumping robot. The jumping robot is composed of a prestretched DE membrane and stiff strip. When DEA is subjected to voltage, the jumping robot is in a flat state. Once the voltage is removed, it will immediately return to the bent state, leading to jump motions (5 cm, a full body length).

DEA has also been used in the exploration of flying robots based on the bioinspired flapping mechanism. In the early efforts, Pelrine et al.[125] designed a thorax-type flapping robot based on the stacked DEA. In a recent work, Lau et al.[137] developed a bioinspired flapping-wing robot. A rolled DEA was assembled into a lightweight shell made of carbon fiber-reinforced polymer (CFRP) to maintain prestretch and increase overall work density. Although the theoretical working density of 30.9% is achieved, the wing can only produce a stroke of 5°–10° when using BJB-TC5005 membrane. Zhao et al.[138] tested a DEMES rotary joint and applied it into a flapping wing. At the

Table 3. Summary of walking/crawling robots.

Speed	Size and weight	Operation situation	Untethered	Reference
35 mm s^{-1}			Yes	[125]
136 mm s^{-1}	180 mm × 180 mm × 100 mm; 292 g	5.5 kV, 7 Hz	No	[76]
70 mm s^{-1}	200 mm × 150 mm; 220 g		Yes	[126]
30 mm s^{-1}	150 mm × 106 mm × 48 mm; 35 g	3.5 kV, 2 Hz	No	[127]
52 mm s^{-1}	150 mm × 54 mm × 55 mm; 20 g	3.5 kV, 7 Hz	No	[205]
4.16 mm s^{-1}		Ramping voltage to 6 kV	Yes	[128]
Wall-climbing 63.43 mm s^{-1}; horizontal planes 88.46 mms^{-1}		6 kV, 16 Hz	No	[129]
		6 kV, 23 Hz		
26.3 mm s^{-1}		6 kV, 20 Hz	No	[74]
161 mm s^{-1}	5 g	9 kV, 16 Hz	No	[130]
Tethered 30 mm s^{-1}; untethered 12 mm s^{-1}	40 mm; tethered 0.19 g, untethered 0.97 g	450 V, 450 Hz	Yes	[131]
518.3 mm s^{-1}	85 mm × 48 mm × 60 mm; 6.5 g	5.5 kV, 17 Hz	No	[132]
5.75 mm s^{-1}		3 kV	No	[206]
2.86 mm s^{-1}		7.5 kV, 0.5 Hz	No	[63]
1.1 mm s^{-1}		17 kV, 0.3 Hz	No	[207]
5.3 mm s^{-1}	170 mm; 10.3 g	2 kV, 2 Hz	No	[208]

frequency of 5 Hz, each joint can achieve more than 60° deformation. However, these prototypes only demonstrate this kind of flight mechanism and cannot actually fly. Recently, Chen et al.[24] presented a flying robot driven by multilayered DEAs, as shown in **Figure 5**f. The weight and resonance frequencies are 100 mg and 500 Hz, respectively. The use of soft actuators makes the flying robot have the advantages of inflight self-sensing and robustness to collisions. This work also highlights that soft actuators can be used to achieve controllable flight because it can provide sufficient bandwidth and power density. Further, Chen et al.[139] demonstrated the novel flying capabilities of the improved flying robot, such as hovering flight, high ascending speed (70 cm s^{-1}), in-flight collision recovery, and somersault. These insect-like flight capabilities have not been achieved by a rigid-powered microaerial vehicle.

Alternatively, Jordi et al.[140] presented a fish-like airship which was propelled by the planar DEA. It can move forward in the air at a speed of 0.45 m s^{-1}. Shintake et al.[104] developed a foldable antagonistic actuator and embedded it in a microair vehicle as elevon. The angular displacement and torque of the actuator can reach ± 26° and 2720 mN mm, respectively. It was successfully demonstrated to provide stable flight control.

3.4. Swimming Robots

Recently, the development of biomimetic swimming robots has become more attractive due to the density of DEs close to that of water. Many kinds of swimming robots driven by DEA have been developed, as shown in **Figure 6**. Inspired by jellyfish, Godaba et al.[141] designed a swimming robot that consists of an air chamber covered by a DE membrane and a bell. When DEA is subjected to voltage, DE membrane is inflated, leading to the increase in buoyancy. Meanwhile, the water inside the bell is ejected, promoting the robot to move upward. Yang et al.[142] presented a swimming robot mimicking cuttlefish. The cone DEA was used as the jet actuated structure. Different from the preset control strategy of the previous swimming robot, the control strategy of this swimming robot is optimized by reinforcement learning. Through reinforcement learning, swimming speed increased by 91%, up to 21 mm s^{-1} (0.38 body length/second). Liu et al.[143] also designed a swimming robot with a fully integrated onboard system based on the buoyant force mechanism. A pressure sensor is used for feedback in closed-loop control, and the robot can move to and stabilize at a specified depth. Further, Cheng et al.[144] developed an untethered soft robotic jellyfish with high mobility. The maximum speed the robot can reach is around 0.5 cm s^{-1}. If the robot is not embedded with a power source, the peak speed can up to 1 cm s^{-1}. Shintake et al.[145] introduced two kinds of biomimetic swimming robots. A jellyfish and a fish were fabricated by laminating silicone layers to ensure the robots can operate reliably in water. Berlinger et al.[146] designed an autonomous underwater vehicle (AUV) driven by a fin-like DEA. All the electronic components were put into a 3D-printed body. The thrust force of the fin can be easily adjusted by controlling the number of actuation layers, and the AUV can swim at a speed of 0.55 body lengths per second under the highest thrust force. In another

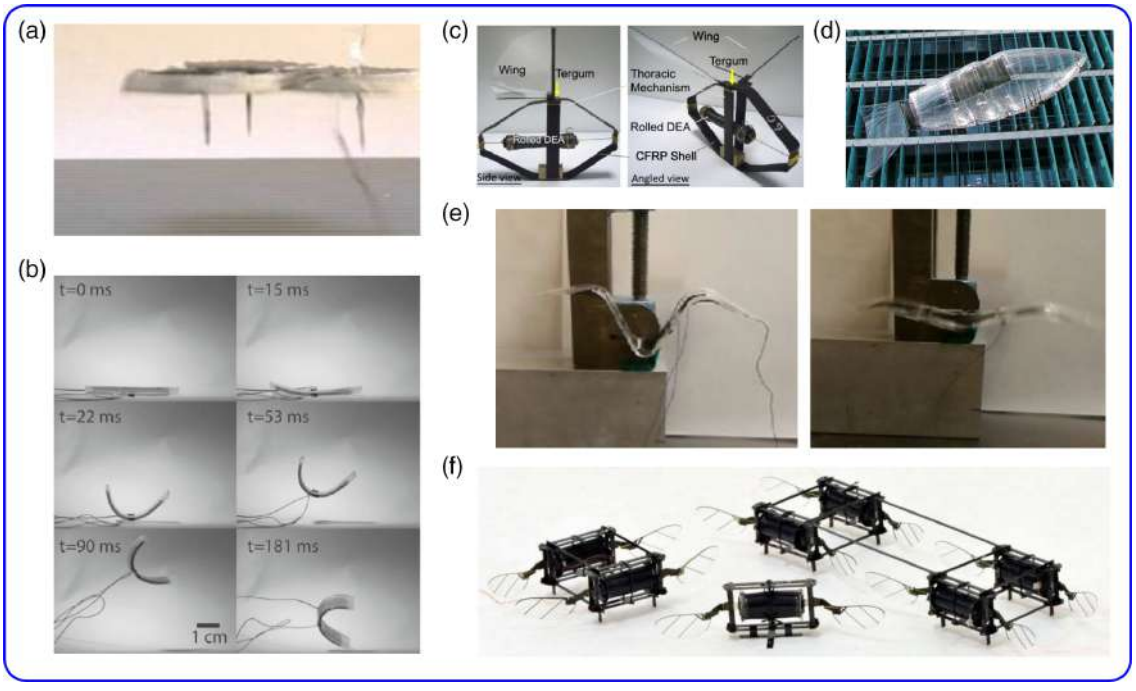

Figure 5. Jumping/flying robots. a) Hopping robots. Reproduced with permission.[135] Copyright 2004, SPIE. b) Jumping robots. Reproduced with permission.[136] Copyright 2019, IOP Publishing. c) Flapping-wing robots. Reproduced with permission.[137] Copyright 2014, IOP Publishing. d) Fish-like airship. Reproduced with permission.[140] Copyright 2010, IOP Publishing. e) DEMES rotary joint-based flapping wing. Reproduced with permission.[138] Copyright 2015, Springer Nature. f) Flying robot. Reproduced with permission.[24] Copyright 2019, Springer Nature.

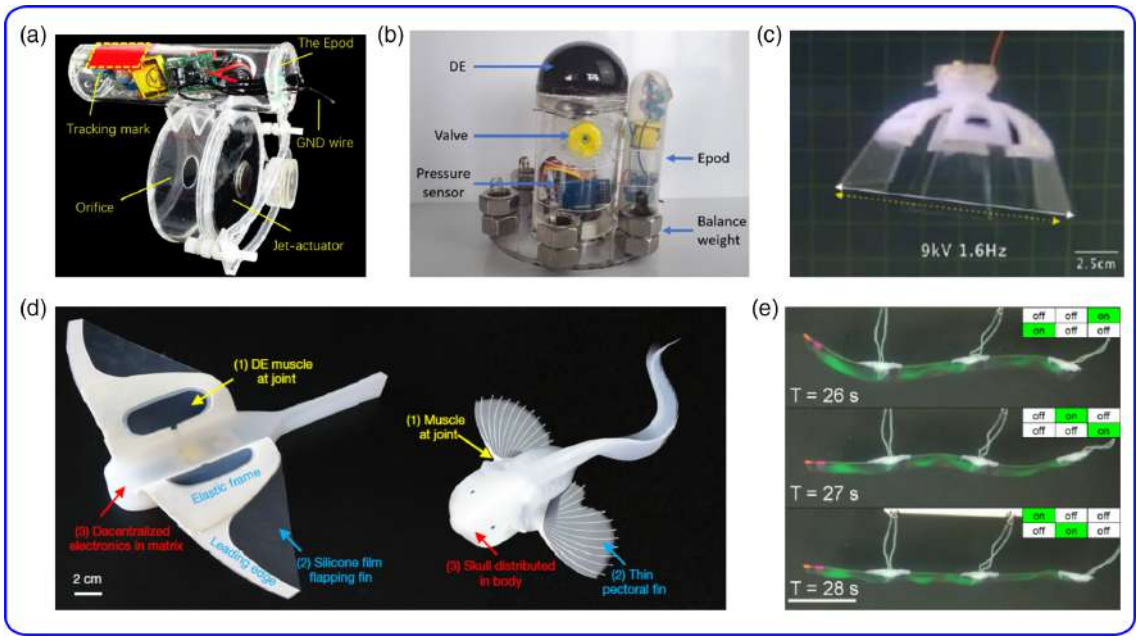

Figure 6. Swimming robots. a) A swimming robot mimicking cuttlefish. Reproduced with permission.[142] Copyright 2018, Springer Nature. b) A swimming robot based on the buoyant force mechanism. Reproduced with permission.[143] Copyright 2017, ASME. c) An untethered soft robotic jellyfish. Reproduced with permission.[144] Copyright 2019, IOP Publishing. d) Deep-sea soft robot. Reproduced with permission.[149] Copyright 2021, Springer Nature. e) A swimming robot inspired by leptocephali. Reproduced with permission.[150] Copyright 2018, The American Association for the Advancement of Science.

work, Tang et al.[147] proposed a frog-inspired robot. The leg and feet of the robot were fabricated using a two-segmented DEMES. By imitating the real frog movement, the robot can swim at a speed of 19 mm s^{-1}. Inspired by Mobula, Li et al.[148] developed a soft fish driven by DEA. Transparent conductive hydrogel and the surrounding water were used as the positive electrode and electric ground, respectively, enabling the fish to sail in stealth sailing. With the integrated onboard system, the speed of the fish reached 6.4 cm s^{-1} (0.69 body length/second). Recently, the same group developed an untethered soft robot for deep-sea exploration.[149] The robot successfully achieved a flapping angle of 6.3° when the AC voltage was 9 kV at 0.5 Hz at a depth of 10 900 m in the Mariana Trench (11.33° N, 142.19° E). Actuated by AC voltage of 8 kV at 1 Hz, it can also swim freely at a speed of 5.19 cm s^{-1} (0.45 body length/second) at a depth of 3224 m in the South China Sea (18.23° N, 114.13° E). It proves that the soft robot has the potential to be applied in extreme environments. Christianson et al.[150] presented a swimming robot inspired by leptocephali. The robot is frameless, and both electrodes were fluids. It makes the swimming robot translucent (transmittance of 94%). The robot moves forward by undulatory swimming, and the maximum speed is 1.9 mm s^{-1}. The performance and characteristics of swimming robots are compared in **Table 4**.

3.5. Humanoid Robots

Making a humanoid robot is one of the most challenging issues in robot researches. As one of the most promising materials due to the similar capability of natural muscle, such as actuation strain, actuation density, and response time, various humanoid robots have been designed and tested based on DEAs, as shown in **Figure 7**.

In the early stage, Kovacs et al.[151] developed an arm-wrestling robot. Based on the mechanism of human agonist–antagonist muscle, more than 250 rolled DEAs were arranged in two groups. Although the robot lost in the arm-wrestling contest, it still shows the potential of DE as artificial muscle. Later, Lu et al.[152] developed a bioinspired artificial arm based on a linear DEA. With the help of suitable stiff fibers arranged in the horizontal direction to maintain large prestretch, the linear DEA can achieve strain up to 142%, allowing it to imitate slender natural muscle. The forearm of the artificial arm can rotate 70° relative to the upper arm when voltage is applied to the linear DEA. Duduta et al.[26] also demonstrated the muscle-like actuation of stacked DEA in an artificial arm.

In contrast, researchers have made several efforts to mimic human facial expressions using DEAs. Wang and coworkers[153,154] used DEAs to drive a robotic skull. Two DEAs were used to connect the upper and lower jaws. Using feedforward control, it can mimic jaw movement very well. In addition, some efforts have also been spent to imitate human eyeball movements. Carpi et al.[155] used two stacked DEAs arranged in the configuration of agonist–antagonist to imitate the rectus-type human ocular muscles. The eyeball can reach the maximum rotation of ±25°. Alternatively, Liu et al.[156] demonstrated the eye movement with an inflated DEA. Compared with the uninflated one, the inflated DEA can produce a larger rotation angle. In another recent

Table 4. Summary of swimming robots.

Speed	Thrust	Size and weight	Operation situation	Untethered	Reference
≈11 mm s^{-1}	0.15 N	2.56 N	5 kV	No	[141]
21 mm s^{-1}		Diameter 95 mm, height 55 mm; 126 g.	6.8 kV	Yes	[142]
3.5 cm s^{-1}		Diameter 60 mm, height 100 mm; 0.45 kg	10 kV	Yes	[143]
Tethered 10 mm s^{-1}, untethered 5 mm s^{-1}	0.00012 N		9 kV, 1.6 Hz	Yes	[144]
Fish ≈8 mm s^{-1}	Fish 0.5 mN	Fish 120 mm; 3.8 g	Fish 3 kV, 3 Hz	No	[145]
Jellyfish ≈1.5 mm s^{-1}	Jellyfish 0.25 mN	Jellyfish diameter 61 mm; 2.6 g	Jellyfish 3 kV, 2 Hz		
55 mm s^{-1}	25 mN	100 mm × 60 mm × 30 mm; 115 g	2 kV, 2.2 Hz	Yes	[146]
19 mm s^{-1}	0.078 N	108 g	5 kV, 0.25 Hz	No	[147]
64 mm s^{-1}		Body length 93 mm, 90.3 g	9 kV, 5 Hz	Yes	[148]
51.9 mm s^{-1}		Long 22 cm, wingspan 28 cm	8 kV, 1 Hz	Yes	[149]
1.9 mm s^{-1}	42 ± 7 mN	220 mm × 50 mm × 15 mm, 25.1 g	7.5 kV, 0.33 Hz	No	[150]
37.2 mm s^{-1}		Length 150 mm, thickness 0.75 mm; 4.4 g	5 kV, 0.75 Hz	No	[209]
33 mm s^{-1}		0.076 m × 0.072 m × 0.056 m, 54 g	5 kV, 15 Hz	No	[210]

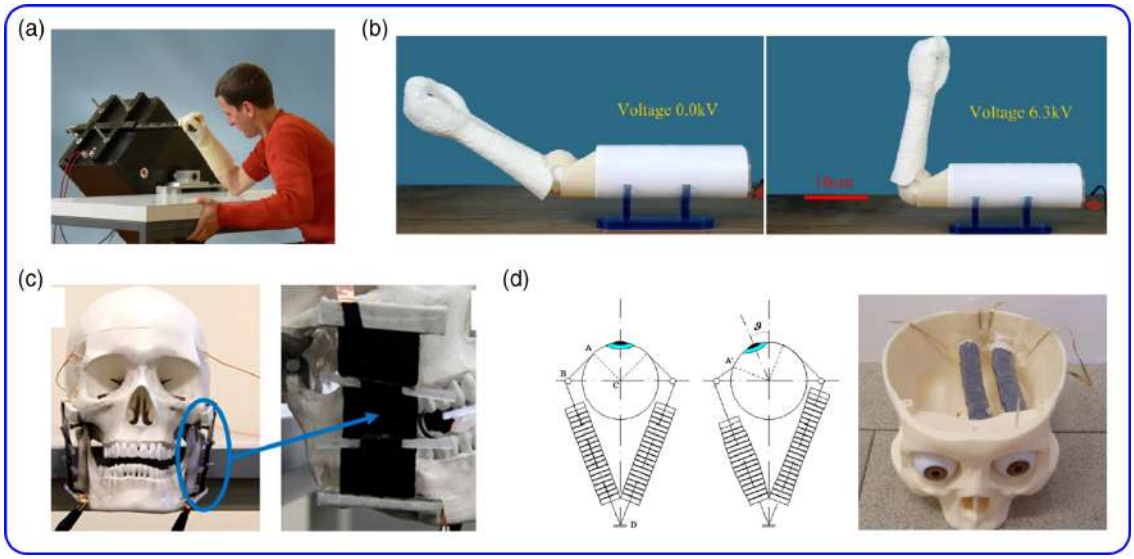

Figure 7. a) Arm-wrestling robot. Reproduced with permission.[151] Copyright 2007, IOP Publishing. b) Artificial arm. Reproduced with permission.[152] Copyright 2016, Elsevier. c) DEA-driven jaw. Reproduced with permission.[154] Copyright 2016, Elsevier. d) Stacked DEA-driven eyeball. Reproduced with permission.[155] Copyright 2007, IOP Publishing.

work, Li et al.[157] combined three spring roll DEAs together to realize vertical, horizontal, and circular motions. By controlling the voltage of the three spring roll DEAs, the eyeball can track desired trajectories effectively. These works will contribute to the development of bioinspired humanoid robots.

3.6. Tunable Lens for Soft Robots

In addition to basic motion functions, the visual system is also an important part of robotic systems. Tunable lens based on DEA is a promising technology for visual systems, thanks to its simple structure. It can tune the focal length by changing the shape of the lens or the refractive index of the optical medium, instead of adjusting the distance like traditional focus tunable lens structures. Inspired by the architecture of the ciliary muscle and crystalline lens of the human eye, Carpi et al.[158] designed an electrically tunable lens that consists of a ring-shaped DEA and a fluid-filled lens, as shown in **Figure 8**a. When applied a voltage, the annular DEA deforms the lens, leading to the change of focal length. Ghilardi et al.[159] replaced the fluid-filled elastomeric lens with a soft silicone lens and divided the surrounding actuating region into four parts. By applying different voltage combinations to the DEA, the lens can deform in a specific direction so as to adjust the defocus or astigmatism. Shian et al.[160] present a new

structure of adaptive lens. The lens consists of a frame mounted both sides by an active DE membrane and a passive membrane, respectively, and a clear liquid filled the lens cavity. The focal length can change over 100% with response time less than 1 s. Recently, Li et al.[161] proposed a new mode of human–machine interface. To mimic the working mechanisms of human eyes, a fluid-filled lens was assembled into a cone DEA in the antagonistic configuration with multiple degrees of freedom. The deformation and motion of the fluid-filled lens were controlled by the electrooculographic signals generated by the eye movements.

3.7. Tactile Displays for Soft Robots

Tactile perception could make the interaction between robots and unstructured environments or humans safer. DEA-based tactile displays have been studied for many years. Koo et al.[162] proposed the first tactile display based on DEAs. The device is in the configuration of 4×5 actuator array. With a 3.5 kV input voltage, the actuator can achieve a maximum displacement of 471 μm, which is sufficient as a tactile display device. Later, the same research group proposed a liquid coupling tactile display,[163] as shown in **Figure 9**a. Between the actuator and the touch spot, liquid coupling was used as the force transmission to ensure the operation safety for users. The tactile display can achieve a force of over 40 mN to simulate the figure tip. At the frequency of 3−10 Hz, the displacements were about 240–120 μm, which meet the requirements of frequency for simulating the Meissner corpuscles as well as the Merkel cells. Alternatively, Matysek et al.[164] designed a tactile display using multilayer DEA. The tactile display consists of a 3×3 actuator matrix, and each actuator has a size of 5 mm × 5 mm. The interactive information between users and tactile display can be easily obtained by measuring the actual capacitance and realize tactile feedback. Based on the evidence that humans are very sensitive to the distributions of shear force, Knoop et al.[165] proposed a new shear tactile display. When a voltage is applied, this device converts the in-plane movement of DEAs into the lateral motion of tactile elements directly to apply shear forces to skin. Marette et al.[166] designed a flexible haptic display operating at 1 kV. The haptic display consists of a 4×4 matrix independent DEA and flexible high-voltage thin-film transistors (HVTFTs). The state of each DEA can be independently switched by applying a gate voltage of 30 V on its associated HVTFT. Recently, more remarkable achievements have been made on tactile display. Yun et al.[167] developed a soft and transparent visuo–haptic interface composed of DE microactuator (DEMA) arrays and a touch-sensitive visual display. DEMA was designed into multiple 3D structures for programmable control, and AgNWs were used as compliant electrodes to ensure high transmittance (up to 90%). Thanks to the 3D structure, DEMA deforms in the vertical direction and outputs sufficient normal force (up to 130 mN at a voltage of 20 MV m^{-1} and a frequency of 240 Hz). DEMA also exhibits fast response and high durability, so that it can be used in the human tactile interface. Ji et al.[168] developed an untethered feel-through haptics. Thanks to the extremely thin thickness of the active layers, the weight of the multilayer DEA can be ignored and the multilayer DEA can be driven by sub-500 V voltage. With compact lightweight (1.3 g) on-board electronics, the device can generate rich vibrotactile feedback at frequencies from 1 to 500 Hz. Zhao et al.[169] proposed a wearable haptic communication device that consists of a linear DEA array. The linear DEA transmits information by deforming skin at a broad bandwidth (10–200 Hz). Human testing has shown that the actuation can be easily perceived on the forearm.

4. Challenges and Perspectives

Various applications of DEAs in soft robots have been introduced in this article. From these discussions, we can infer that DEA is very promising for soft robots. Although researchers have made extensive efforts and achieved remarkable results in the past decade, there are still many challenges for the real-world applications of DEAs. In this section, we will review the main challenges of DEAs and their applications for future work.

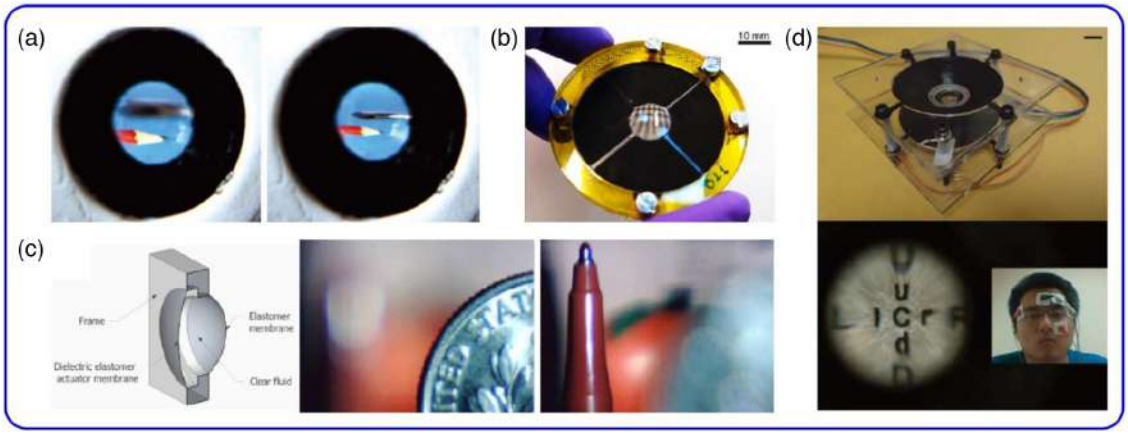

Figure 8. a) Fluid-filled elastomeric lens. Reproduced with permission.[158] Copyright 2011, John Wiley and Sons. b) Tunable optical lens. Reproduced with permission.[159] Copyright 2019, Springer Nature. c) Adaptive lens. Reproduced with permission.[160] Copyright 2013, OSA Publishing. d) Human−machine interface. Reproduced with permission.[161] Copyright 2019, John Wiley and Sons.

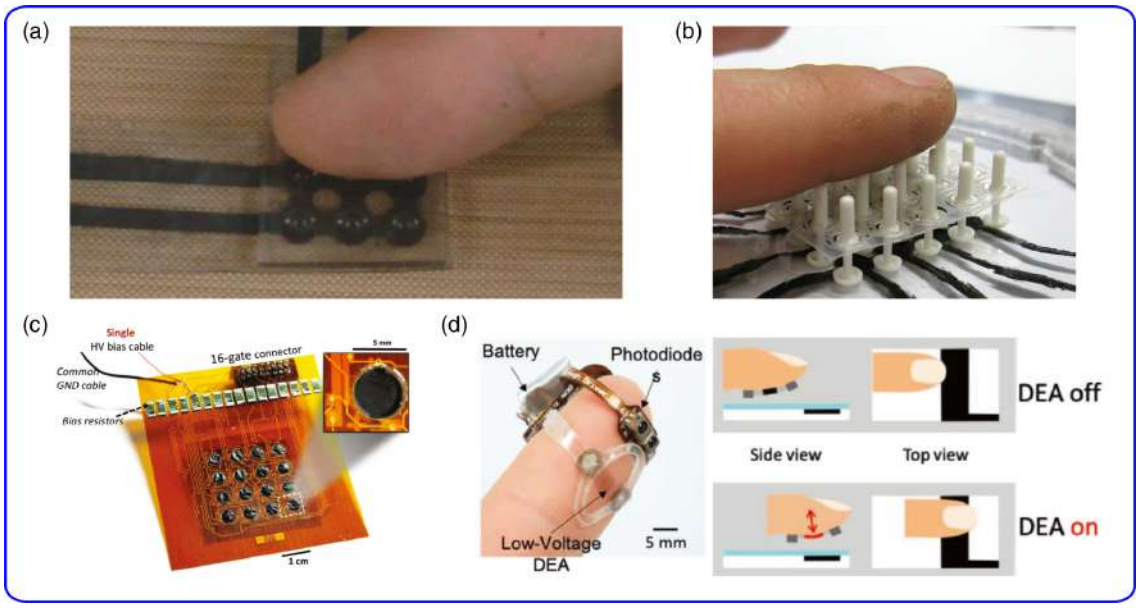

Figure 9. a) Liquid coupling tactile display. Reproduced with permission.[163] Copyright 2014, Elsevier. b) Shear tactile display. Reproduced with permission.[165] Copyright 2014, SPIE. c) Flexible haptic display. Reproduced with permission.[166] Copyright 2017, John Wiley and Sons. d) Untethered feel-through haptics. Reproduced with permission.[168] Copyright 2020, John Wiley and Sons.

4.1. Design

The biological evolutionary law of the survival of the fittest provides a better direction for the development of soft robots. The body structure of natural creatures evolved to adapt to the environment could provide invaluable insights for the design of DEAs and soft robots, especially for those working in extreme environments. From the previous discussion, it can be seen that many swimming robots are untethered, while walking/crawling robots are generally tethered. This is due to the trade-offs made by researchers among many parameters. For instance, additional constraints, such as the weight and size of the power system, must be considered when designing crawling or flying robots due to the lower output force of the actuator. However, the additional weight is not a major problem in the swimming robot, because the weight can be balanced by buoyancy. Thus, good trade-offs should be made to obtain the best performance for soft robots depending on the application.

To achieve the autonomous operation of robots, a sensing system is needed. The traditional sensing system is rigid, which is not applicable for soft robots with large deformation. Even the flexible sensor will cause constraints to the soft robots. As discussed in Section 2.4, DEA has the self-sensing capability. However, the related research is still insufficient. It will be an interesting direction to design DEAs and soft robots with self-sensing functions.

4.2. Operating Voltage

Generally, the voltage used to drive DEAs is up to several kilovolts. This greatly limits the application of DEAs, especially in wearable devices, although the required current is very low (less than 1 mA). To reduce the driving voltage, the most effective method is to decrease the thickness of DE membrane. In experiments, DE membrane (VHB4910 or VHB4905) is often prestretched to reduce the thickness. The prestretch allows DEAs to produce larger voltage-induced deformation, while also suppresses the occurrence of electromechanical instability. However, the prestretch of the DE membrane requires a rigid frame to be maintained, which limits the flexibility of DEA. The viscoelasticity of the VHB also significantly affects the response time of DEA. To overcome these limitations, many researchers use silicone such as Sylgard 184, Ecoflex 0030, etc., to make DE membrane. These kinds of elastomers exhibit hyperelasticity and can work at a very high frequency, thanks to their low viscoelasticity. Based on the pad-printing technique, a 3 μm-thick DE membrane was produced. It can achieve a lateral strain of 7.5% at a voltage of 245 V.[170] The stacked DEA is popular as it does not require prestretch. By spin coating, Zhao et al.[111] designed a compact DEA with multilayer stacked sheets (25 μm per layer). It can be operated at 200 Hz. These fabrication technologies make it possible to manufacture low-voltage DEAs, which is great progress in developing DEA-based soft robots. Next, researchers should make more efforts to make low-voltage DEAs through the use of new kinds of DE materials.

4.3. Control

Such a high voltage to drive DEA is usually provided by an external high-voltage amplifier, which also means that DEA or its application is tethered. This is often a disadvantage that prevents it from operating independently, such as crawling robots and flying robots. Making a small, lightweight circuit board that can be integrated into a soft robot to enable it to move autonomously is

an urgent issue that researchers have to consider. It should be noted that small voltage amplifiers (EMCO products) powered by low voltage battery have also been used to drive untethered robots recently. For example, the small voltage amplifiers (A Series, EMCO) used in literature[146,171,172] have a maximum size of 6.35 mm × 11.43 mm × 33.78 mm and a maximum weight of 8.49 g and enable it to be integrated into a circuit board. The output high voltage is up to 6 kV. However, the low bandwidth can only allow DEA to operate at a lower frequency. In contrast, the composition of high-voltage electronic components is much more complicated than that of low voltage. Once many DEAs independently are controlled, high-voltage control components such as relays will significantly increase the weight and volume, and the voltage applied to each DEA cannot be adjusted independently. If multiple small voltage amplifiers are used, the cost will be very high. Therefore, the development of low-voltage-driven DEA is still the main task in the field of DEs. It should also be noted that the artificial nervous system used to replace the conventional hard control components can also be directly assembled into a soft robot, as mentioned previously.[133] This kind of control system provides a new solution for the development of soft robots.

In addition, the control strategy is also a huge challenge for DEA-based soft robots due to the nonlinear deformation, viscoelastic hysteresis, electromechanical instability, etc. In recent years, researchers have done some work to address this challenge and feedforward control is proved to be a promising approach.[42,153,173,174] Zou et al.[42] have proved that DEAs can be finely controlled by a feedforward control approach. To mimic human jaw movement, Gupta et al.[153] developed a feedforward controller based on the nonlinear dynamic model. In addition, feedback control,[175,176] reinforcement learning,[142] etc. also were used in the control strategy. However, unlike traditional rigid robots, soft robots have more degrees of freedom and soft robots with different structures have different forms of nonlinearity. Most of the existing control theories are not applicable to DEA-based soft robots. Hence, more efforts are still needed in the control theory of soft robots.

4.4. Reliability

Reliable actuation without undergoing failure, such as electromechanical instability or dielectric breakdown, is necessary for the commercial application of DEA-driven soft robots. First, the materials used in DEAs must have stable performance. Due to the existence of viscoelasticity, VHB will exhibit viscoelastic relaxation under the action of prestretch, and the contraction force in the membrane will decrease after complete relaxation. Silicone rubber is a good choice due to its more reliable performance. However, its smaller voltage-induced strain is a factor that has to be considered when using this material to make DEAs. In contrast, compliant electrodes are also very important factors. The most commonly used carbon grease has a short lifetime and will dry for a long time.[177] It is also difficult to integrate DEAs using carbon grease with other structures due to its good fluidity. Alternatively, carbon black and CNTs are often directly used in multilayer stacked DEAs. They can also be mixed into silicone matrix and pad printed on the surface of DE membrane for curing.[107] In addition, Araromi et al.[39] proposed a new approach for the compliant electrodes with high-resolution patterns and robust adhesion. The PDMS–carbon compliant electrodes were patterned by laser ablation and boned with PDMS membrane by oxygen plasma activation. These compliant electrodes and fabrication methods provide robust adhesion between the compliant electrodes and the DE membrane, which improve the stability of DEA.

The lifetime is a key parameter of DEA, and it is necessary to study fatigue properties, because most DEAs work under cyclic voltage loading. Some reported lifetimes of DEA are shown in Table 2. In previous research, Rosset et al.[107] demonstrated a DEA-driven motor, which has accumulated several tens of millions of cycles in two years and can still work perfectly. The rolling robot based on this kind of motor travelled a distance of 25.8 km (61% of the total marathon distance). Although the DEA used in the flying robot has a lifetime of over 600 000 cycles, it still has to be improved.[24] After all, the working frequency reaches several hundred hertz. In a recent work, it has been shown that the choice of compliant electrode and the application method has a significant effect on the high-cycle electromechanical aging of DEA.[172] However, these studies only tested the lifetime of DEAs and did not study the degradation mechanism. In future work, it is necessary to further study the degradation mechanism of DEAs to improve stability and durability.

5. Conclusion

In this work, some highlights of research in DEAs are reviewed. First, the working principle and the typical configuration of DEAs are described. Then various applications of DEAs are classified and discussed, including soft grippers, walking/crawling robots, jumping/flying, swimming robots, humanoid robots, tunable lens, and tactile displays. In addition, there are also some potential applications that are not described in detail here, such as micropumps,[178–180] vibration devices,[181] loudspeakers,[182,183] cell manipulation in biology,[184–186] dynamic liquid droplet manipulation,[187] etc. Beyond the application as actuators, DEs can also be used as energy harvesters and sensors.[36–39,188–190] From these discussions, we can infer that DEA has great potential in the application of soft robots, especially with biologically inspired features. There are still many challenges for DEAs to be used in the real world, although some efforts have been made to address them. Future works should focus on these challenges and truly leverage the advantages of DEAs for soft robots.

Acknowledgements

This work was supported by the National Natural Science Foundation of China (grant no. 11772109).

Conflict of Interest

The authors declare no conflict of interest.

Keywords

control, dielectric elastomer actuators, soft actuators, soft robots

Received: December 28, 2020
Revised: May 8, 2021
Published online:

[1] R. Pelrine, R. Kornbluh, Q. B. Pei, J. Joseph, *Science* **2000**, *287*, 836.
[2] S. Shian, K. Bertoldi, D. R. Clarke, *Adv. Mater.* **2015**, *27*, 6814.
[3] Q. Shen, T. Wang, J. Liang, L. Wen, *Smart Mater. Struct.* **2013**, *22*, 075035.
[4] X. Zhao, *Soft Matter* **2014**, *10*, 672.
[5] C. Yang, Z. Suo, *Nat. Rev. Mater.* **2018**, *3*, 125.
[6] H. Yuk, B. Lu, X. Zhao, *Chem. Soc. Rev.* **2019**, *48*, 1642.
[7] X. Du, H. Cui, T. Xu, C. Huang, Y. Wang, Q. Zhao, Y. Xu, X. Wu, *Adv. Funct. Mater.* **2020**, *30*, 1909202.
[8] Y. Kim, H. Yuk, R. Zhao, S. A. Chester, X. Zhao, *Nature* **2018**, *558*, 274.
[9] W. Hu, G. Z. Lum, M. Mastrangeli, M. Sitti, *Nature* **2018**, *554*, 81.
[10] H. Lu, M. Zhang, Y. Yang, Q. Huang, T. Fukuda, Z. Wang, Y. Shen, *Nat. Commun.* **2018**, *9*, 3944.
[11] J. S. Leng, X. Lan, Y. J. Liu, S. Y. Du, *Prog. Mater. Sci.* **2011**, *56*, 1077.
[12] Q. Peng, H. Wei, Y. Qin, Z. Lin, X. Zhao, F. Xu, J. Leng, X. He, A. Cao, Y. Li, *Nanoscale* **2016**, *8*, 18042.
[13] Y. F. Zhang, N. Zhang, H. Hingorani, N. Ding, D. Wang, C. Yuan, B. Zhang, G. Gu, Q. Ge, *Adv. Funct. Mater.* **2019**, *29*, 1806698.
[14] H. T. Lin, G. G. Leisk, B. Trimmer, *Bioinspir. Biomim.* **2011**, *6*, 026007.
[15] C. Laschi, M. Cianchetti, *Front Bioeng Biotechnol* **2014**, *2*, 3.
[16] T. J. White, D. J. Broer, *Nat. Mater.* **2015**, *14*, 1087.
[17] C. Wang, K. Sim, J. Chen, H. Kim, Z. Rao, Y. Li, W. Chen, J. Song, R. Verduzco, C. Yu, *Adv. Mater.* **2018**, *30*, 1706695
[18] M. Rogóż, H. Zeng, C. Xuan, D. S. Wiersma, P. Wasylczyk, *Adv. Opt. Mater.* **2016**, *4*, 1689.
[19] G. M. Whitesides, *Angew. Chem., Int. Ed.* **2018**, *57*, 4258.
[20] E. Acome, S. K. Mitchell, T. G. Morrissey, M. B. Emmett, C. Benjamin, M. King, M. Radakovitz, C. Keplinger, *Science* **2018**, *359*, 61.
[21] S. K. Mitchell, X. Wang, E. Acome, T. Martin, K. Ly, N. Kellaris, V. G. Venkata, C. Keplinger, *Adv. Sci.* **2019**, *6*, 1900178.
[22] L. An, F. F. Wang, S. B. Cheng, T. Q. Lu, T. J. Wang, *Smart Mater. Struct.* **2015**, *24*, 035006.
[23] T. Li, C. Keplinger, R. Baumgartner, S. Bauer, W. Yang, Z. Suo, *J. Mech. Phys. Solids* **2013**, *61*, 611.
[24] Y. Chen, H. Zhao, J. Mao, P. Chirarattananon, E. F. Helbling, N. P. Hyun, D. R. Clarke, R. J. Wood, *Nature* **2019**, *575*, 324.
[25] C. Cao, X. Gao, A. T. Conn, *Adv. Mater. Technol.* **2019**, *4*, 1900128.
[26] M. Duduta, E. Hajiesmaili, H. Zhao, R. J. Wood, D. R. Clarke, *Proc. Natl. Acad. Sci. U. S. A.* **2019**, *116*, 2476.
[27] G. Kovacs, L. Düring, S. Michel, G. Terrasi, *Sens. Actuators, A* **2009**, *155*, 299.
[28] R. D. Kornbluh, R. Pelrine, Q. Pei, R. Heydt, S. Stanford, S. Oh, J. Eckerle, in *Smart Structures and Materials 2002: Industrial and Commercial Applications of Smart Structures Technologies*, Vol. *4698*, SPIE, San Diego, CA **2002**, p. 254.
[29] O. A. Araromi, I. Gavrilovich, J. Shintake, S. Rosset, M. Richard, V. Gass, H. R. Shea, *IEEE-ASME Trans. Mechatron.* **2015**, *20*, 438.
[30] P. Brochu, Q. Pei, *Macromol. Rapid Commun.* **2010**, *31*, 10.
[31] G. Y. Gu, J. Zhu, L. M. Zhu, X. Zhu, *Bioinspir. Biomim.* **2017**, *12*, 011003.
[32] U. Gupta, L. Qin, Y. Wang, H. Godaba, J. Zhu, *Smart Mater. Struct.* **2019**, *28*, 103002.
[33] W. Liang, H. Liu, K. Wang, Z. Qian, L. Ren, L. Ren, *Adv. Mech. Eng.* **2020**, *12*, 168781402093340.
[34] S. Chen, Y. Cao, M. Sarparast, H. Yuan, L. Dong, X. Tan, C. Cao, *Adv. Mater. Technol.* **2019**, *5*, 1900837.
[35] J. Huang, S. Shian, Z. Suo, D. R. Clarke, *Adv. Funct. Mater.* **2013**, *23*, 5056.
[36] C. L. Zhang, Z. H. Lai, X. X. Rao, J. W. Zhang, D. Yurchenko, *Energy Conv. Manag.* **2020**, *205*, 112351.
[37] G. Moretti, M. Santos Herran, D. Forehand, M. Alves, H. Jeffrey, R. Vertechy, M. Fontana, *Renewable Sustainable Energy Rev.* **2020**, *117*, 109430.
[38] B. Huang, M. Li, T. Mei, D. McCoul, S. Qin, Z. Zhao, J. Zhao, *Sensors* **2017**, *17*, 2708.
[39] O. A. Araromi, S. Rosset, H. R. Shea, *ACS Appl. Mater. Interfaces* **2015**, *7*, 18046.
[40] S. Bauer, S. Bauer-Gogonea, I. Graz, M. Kaltenbrunner, C. Keplinger, R. Schwodiauer, *Adv. Mater.* **2014**, *26*, 149.
[41] W. Hong, *J. Mech. Phys. Solids* **2011**, *59*, 637.
[42] J. Zou, G. Gu, *IEEE Robot. Autom. Lett.* **2019**, *4*, 2340.
[43] H. Godaba, C. C. Foo, Z. Q. Zhang, B. C. Khoo, J. Zhu, *Appl. Phys. Lett.* **2014**, *105*, 112901.
[44] A. O'Halloran, F. O'Malley, P. McHugh, *J. Appl. Phys.* **2008**, *104*, 071101.
[45] S. Rosset, H. R. Shea, *Appl. Phys. A* **2012**, *110*, 281.
[46] S.-H. Low, G.-K. Lau, *Smart Mater. Struct.* **2014**, *23*, 125021.
[47] F. Carpi, P. Chiarelli, A. Mazzoldi, D. De Rossi, *Sens. Actuators, A* **2003**, *107*, 85.
[48] D.-Y. Cho, K. Eun, S.-H. Choa, H.-K. Kim, *Carbon* **2014**, *66*, 530.
[49] S. Shian, R. M. Diebold, A. McNamara, D. R. Clarke, *Appl. Phys. Lett.* **2012**, *101*, 061101.
[50] J. J. Liang, L. Li, K. Tong, Z. Ren, W. Hu, X. F. Niu, Y. S. Chen, Q. B. Pei, *ACS Nano* **2014**, *8*, 1590.
[51] Y. R. Lee, H. Kwon, D. H. Lee, B. Y. Lee, *Soft Matter* **2017**, *13*, 6390.
[52] Y. Gao, X. Fang, D. Tran, K. Ju, B. Qian, J. Li, *R. Soc. Open Sci.* **2019**, *6*, 182145.
[53] C. Keplinger, J.-Y. Sun, C. C. Foo, P. Rothemund, G. M. Whitesides, Z. Suo, *Science* **2013**, *341*, 984.
[54] G. Haghiashtiani, E. Habtour, S.-H. Park, F. Gardea, M. C. McAlpine, *Extreme Mech. Lett.* **2018**, *21*, 1.
[55] P. Le Floch, N. Molinari, K. Nan, S. Zhang, B. Kozinsky, Z. Suo, J. Liu, *Nano Lett.* **2019**, *20*, 224.
[56] C. Xu, B. Li, C. Xu, J. Zheng, *J. Mater. Sci.: Mater. Electron.* **2015**, *26*, 9213.
[57] Y. Bai, Y. Jiang, B. Chen, C. Chiang Foo, Y. Zhou, F. Xiang, J. Zhou, H. Wang, Z. Suo, *Appl. Phys. Lett.* **2014**, *104*, 062902.
[58] Y. F. Goh, S. Akbari, T. V. Khanh Vo, S. J. A. Koh, *Soft Robot.* **2018**, *5*, 675.
[59] M. Kollosche, J. Zhu, Z. Suo, G. Kofod, *Phys. Rev. E Stat. Nonlin. Soft Matter Phys.* **2012**, *85*, 051801.
[60] S. J. A. Koh, C. Keplinger, R. Kaltseis, C.-C. Foo, R. Baumgartner, S. Bauer, Z. Suo, *J. Mech. Phys. Solids* **2017**, *105*, 81.
[61] S. Rosset, O. A. Araromi, H. R. Shea, *Extreme Mech. Lett.* **2015**, *3*, 72.
[62] K. M. Digumarti, C. Cao, J. Guo, A. T. Conn, J. Rossiter, in *2018 IEEE Int. Conf. on Soft Robotics (RoboSoft)*, IEEE, Piscataway, NJ **2018**, p. 303.
[63] L. Qin, J. Cao, Y. Tang, J. Zhu, *J. Appl. Mech.* **2018**, *85*, 051001.
[64] Y. Liu, B. Liu, T. Yin, Y. Xiang, H. Zhou, S. Qu, *Smart Mater. Struct.* **2020**, *29*, 015008.
[65] W. Sun, F. Liu, Z. Ma, C. Li, J. Zhou, *AIP Adv.* **2017**, *7*, 015308.
[66] J. Huang, T. Li, C. Chiang Foo, J. Zhu, D. R. Clarke, Z. Suo, *Appl. Phys. Lett.* **2012**, *100*, 041911.
[67] G. Kovacs, L. Düring, in *Electroactive Polymer Actuators and Devices (EAPAD) 2009*, Vol. *7287*, San Diego, CA **2009**, p. 72870A.
[68] C. T. Nguyen, H. Phung, T. D. Nguyen, C. Lee, U. Kim, D. Lee, H. Moon, J. Koo, J.-d. Nam, H. R. Choi, *Smart Mater. Struct.* **2014**, *23*, 065005.

[69] Z. Li, M. Sheng, M. Wang, P. Dong, B. Li, H. Chen, *Smart Mater. Struct.* **2018**, *27*, 075023.
[70] H. S. Jung, K. H. Cho, J. H. Park, S. Y. Yang, Y. Kim, K. Kim, C. T. Nguyen, H. Phung, P. T. Hoang, H. Moon, J. C. Koo, H. R. Choi, *Smart Mater. Struct.* **2018**, *27*, 075011.
[71] J. Maas, D. Tepel, T. Hoffstadt, *Meccanica* **2015**, *50*, 2839.
[72] F. Carpi, C. Salaris, D. D. Rossi, *Smart Mater. Struct.* **2007**, *16*, S300.
[73] W. Sun, F. Liu, Z. Ma, C. Li, J. Zhou, *J. Appl. Phys.* **2016**, *120*, 084901.
[74] J. Li, L. Liu, Y. Liu, J. Leng, *Soft Robot.* **2019**, *6*, 69.
[75] J. Huang, T. Lu, J. Zhu, D. R. Clarke, Z. Suo, *Appl. Phys. Lett.* **2012**, *100*, 211901.
[76] Q. Pei, M. Rosenthal, S. Stanford, H. Prahlad, R. Pelrine, *Smart Mater. Struct.* **2004**, *13*, N86.
[77] Y. S. Teh, S. J. A. Koh, *Extreme Mech. Lett.* **2016**, *9*, 195.
[78] L. Liu, C. Zhang, M. Luo, X. Chen, D. Li, H. Chen, *Smart Mater. Struct.* **2017**, *26*, 085018.
[79] J.-S. Plante, S. Dubowsky, *Sens. Actuators, A* **2007**, *137*, 96.
[80] G. Moretti, L. Sarina, L. Agostini, R. Vertechy, G. Berselli, M. Fontana, *Actuators* **2020**, *9*, 44.
[81] R. Vertechy, G. Berselli, V. Parenti Castelli, G. Vassura, *J. Intell. Mater. Syst. Struct.* **2009**, *21*, 503.
[82] G. Kofod, M. Paajanen, S. Bauer, *Appl. Phys. A* **2006**, *85*, 141.
[83] H. Imamura, K. Kadooka, M. Taya, *Soft Matter* **2017**, *13*, 3440.
[84] J. W. Zhao, S. Wang, D. McCoul, Z. G. Xing, B. Huang, L. W. Liu, J. S. Leng, *Smart Mater. Struct.* **2016**, *25*, 075016.
[85] J. Wissman, L. Finkenauer, L. Deseri, C. Majidi, *J. Appl. Phys.* **2014**, *116*, 144905.
[86] G.-K. Lau, K.-R. Heng, A. S. Ahmed, M. Shrestha, *Appl. Phys. Lett.* **2017**, *110*, 182906.
[87] L. Maffli, S. Rosset, H. R. Shea, *Smart Mater. Struct.* **2013**, *22*, 104013.
[88] F. Wang, C. Yuan, T. Lu, T. J. Wang, *J. Mech. Phys. Solids* **2017**, *102*, 1.
[89] T. Lu, L. An, J. Li, C. Yuan, T. J. Wang, *J. Mech. Phys. Solids* **2015**, *85*, 160.
[90] H. Zhang, Y. Zhou, M. Dai, Z. Zhang, *J. Intell. Mater. Syst. Struct.* **2018**, *29*, 2522.
[91] T. Wang, J. Zhang, J. Hong, M. Y. Wang, *Soft Robot.* **2017**, *4*, 61.
[92] R. Baumgartner, A. Kogler, J. M. Stadlbauer, C. C. Foo, R. Kaltseis, M. Baumgartner, G. Mao, C. Keplinger, S. J. A. Koh, N. Arnold, Z. Suo, M. Kaltenbrunner, S. Bauer, *Adv. Sci.* **2020**, *7*, 1903391.
[93] Z. Li, J. Zhu, C. C. Foo, C. H. Yap, *Appl. Phys. Lett.* **2017**, *111*, 212901.
[94] J. Rossiter, P. Walters, B. Stoimenov, in *Electroactive Polymer Actuators and Devices (EAPAD) 2009*, Vol. *7287*, San Diego, CA **2009**, p. 72870H.
[95] A. York, J. Dunn, S. Seelecke, *Smart Mater. Struct.* **2010**, *19*, 094014.
[96] S. Hau, G. Rizzello, S. Seelecke, *Extreme Mech. Lett.* **2018**, *23*, 24.
[97] C. Cao, X. Gao, A. T. Conn, *Appl. Phys. Lett.* **2019**, *114*, 011904.
[98] M. Follador, M. Cianchetti, B. Mazzolai, *Meccanica* **2015**, *50*, 2741.
[99] S. Nalbach, R. M. Banda, S. Croce, G. Rizzello, D. Naso, S. Seelecke, *Front. Robot. AI* **2020**, *6*, 150.
[100] F. Branz, A. Francesconi, *Smart Mater. Struct.* **2016**, *25*, 095040.
[101] N. Wang, C. Cui, B. Chen, H. Guo, X. Zhang, *J. Mech. Robot.* **2019**, *11*, 041011.
[102] P. Lochmatter, G. Kovacs, *Sens. Actuators, A* **2008**, *141*, 577.
[103] P. Chouinard, J.-S. Plante, *IEEE-ASME Trans. Mechatron.* **2012**, *17*, 857.
[104] J. Shintake, S. Rosset, B. E. Schubert, D. Floreano, H. R. Shea, *IEEE-ASME Trans. Mechatron.* **2015**, *20*, 1997.
[105] M. Hill, G. Rizzello, S. Seelecke, *Smart Mater. Struct.* **2018**, *27*, 025019.
[106] I. A. Anderson, T. Hale, T. Gisby, T. Inamura, T. McKay, B. O'Brien, S. Walbran, E. P. Calius, *Appl. Phys. A* **2009**, *98*, 75.
[107] S. Rosset, H. R. Shea, in *Electroactive Polymer Actuators and Devices (EAPAD) 2015*, Vol. *9430*, San Diego, CA **2015**, p. 943009.
[108] A. Minaminosono, H. Shigemune, Y. Okuno, T. Katsumata, N. Hosoya, S. Maeda, *Front0 Robot. AI* **2019**, *6*, 1.
[109] N. Wang, H. Guo, B. Chen, C. Cui, X. Zhang, *Smart Mater. Struct.* **2019**, *28*, 065013.
[110] R. Wache, D. N. McCarthy, S. Risse, G. Kofod, *IEEE-ASME Trans. Mechatron.* **2015**, *20*, 975.
[111] H. Zhao, A. M. Hussain, M. Duduta, D. M. Vogt, R. J. Wood, D. R. Clarke, *Adv. Funct. Mater.* **2018**, *28*, 1804328.
[112] X. H. Zhao, Z. G. Suo, *Appl. Phys. Lett.* **2007**, *91*, 061921.
[113] Q. Pei, R. Pelrine, S. Stanford, R. Kornbluh, M. Rosenthal, *Synth. Met.* **2003**, *135–136*, 129.
[114] T. A. Gisby, B. M. O'Brien, I. A. Anderson, *Appl. Phys. Lett.* **2013**, *102*, 193703.
[115] S. Rosset, B. M. O'Brien, T. Gisby, D. Xu, H. R. Shea, I. A. Anderson, *Smart Mater. Struct.* **2013**, *22*, 104018.
[116] K. Jung, K. J. Kim, H. R. Choi, *Sens. Actuators, A* **2008**, *143*, 343.
[117] M. Landgraf, U. Zorell, T. Wetzel, S. Reitelshöfer, I. S. Yoo, J. Franke, in *Electroactive Polymer Actuators and Devices (EAPAD) 2015*, Vol. *9430*, San Diego, CA **2015**, 943014.
[118] G. Kofod, W. Wirges, M. Paajanen, S. Bauer, *Appl. Phys. Lett.* **2007**, *90*, 081916.
[119] Y. Wang, U. Gupta, N. Parulekar, J. Zhu, *Sci. China: Technol. Sci.* **2018**, *62*, 31.
[120] J. Shintake, S. Rosset, B. Schubert, D. Floreano, H. Shea, *Adv. Mater.* **2016**, *28*, 231.
[121] J. Shintake, B. Schubert, S. Rosset, H. Shea, D. Floreano, in *2015 IEEE/RSJ Int. Conf. on Intelligent Robots and Systems (IROS)*, Hamburg, Germany **2015**, 1097.
[122] B. Aksoy, H. Shea, *Adv. Funct. Mater.* **2020**, *30*, 2001597.
[123] M. Zhang, G. Li, X. Yang, Y. Xiao, T. Yang, T.-W. Wong, T. Li, *Smart Mater. Struct.* **2018**, *27*, 095016.
[124] J. Eckerle, S. Stanford, J. Marlow, R. Schmidt, S. Oh, T. Low, S. V. Shastri, in *Smart Structures and Materials 2001: Industrial and Commercial Applications of Smart Structures Technologies*, Vol. *4332*, Newport Beach, CA **2001**, p. 269.
[125] R. Pelrine, R. D. Kornbluh, Q. Pei, S. Stanford, S. Oh, J. Eckerle, R. J. Full, M. A. Rosenthal, K. Meijer, in *Smart Structures and Materials 2002: Electroactive Polymer Actuators and Devices (EAPAD)*, Vol. *4695*, San Diego, CA **2002**, p. 126.
[126] Q. Pei, R. Pelrine, S. Stanford, R. D. Kornbluh, M. S. Rosenthal, K. Meijer, R. J. Full, in *Smart Structures and Materials 2002: Industrial and Commercial Applications of Smart Structures Technologies*, Vol. *4698*, San Diego, CA **2002**, p. 246.
[127] C. T. Nguyen, H. Phung, T. D. Nguyen, H. Jung, H. R. Choi, *Sens. Actuators, A* **2017**, *267*, 505.
[128] J. Cao, L. Qin, J. Liu, Q. Ren, C. C. Foo, H. Wang, H. P. Lee, J. Zhu, *Extreme Mech. Lett.* **2018**, *21*, 9.
[129] G. Gu, J. Zou, R. Zhao, X. Zhao, X. Zhu, *Sci. Robot.* **2018**, *3*, eaat2874.
[130] T. Li, Z. Zou, G. Mao, X. Yang, Y. Liang, C. Li, S. Qu, Z. Suo, W. Yang, *Soft Robot.* **2018**, *6*, 133.
[131] X. Ji, X. Liu, V. Cacucciolo, M. Imboden, Y. Civet, A. E. Haitami, S. Cantin, Y. Perriard, H. Shea, *Sci. Robot.* **2019**, *4*, eaaz6451.
[132] J. Zhao, J. Zhang, D. McCoul, Z. Hao, S. Wang, X. Wang, B. Huang, L. Sun, *Soft Robot.* **2019**, *6*, 713.
[133] E. M. Henke, S. Schlatter, I. A. Anderson, *Soft Robot.* **2017**, *4*, 353.
[134] E. M. Henke, K. E. Wilson, I. A. Anderson, *Bioinspir. Biomim.* **2018**, *13*, 046009.
[135] Q. Pei, R. Pelrine, M. A. Rosenthal, S. Stanford, H. Prahlad, R. D. Kornbluh, in *Smart Structures and Materials 2004:*

Electroactive Polymer Actuators and Devices (EAPAD), Vol. *5385*, San Diego, CA **2004**, p. 41.
[136] M. Duduta, F. C. J. Berlinger, R. Nagpal, D. R. Clarke, R. J. Wood, F. Z. Temel, *Smart Mater. Struct.* **2019**, *28*, 09lt01.
[137] G.-K. Lau, H.-T. Lim, J.-Y. Teo, Y.-W. Chin, *Smart Mater. Struct.* **2014**, *23*, 025021.
[138] J. Zhao, J. Niu, D. McCoul, J. Leng, Q. Pei, *Meccanica* **2015**, *50*, 2815.
[139] Y. Chen, S. Xu, Z. Ren, P. Chirarattananon, *IEEE Trans. Robot.* **2021**, https://doi.org/10.1109/tro.2021.30536471.
[140] C. Jordi, S. Michel, E. Fink, *Bioinspir. Biomim.* **2010**, *5*, 026007.
[141] H. Godaba, J. Li, Y. Wang, J. Zhu, *IEEE Robot. Autom. Lett.* **2016**, *1*, 624.
[142] T. Yang, Y. Xiao, Z. Zhang, Y. Liang, G. Li, M. Zhang, S. Li, T. W. Wong, Y. Wang, T. Li, Z. Huang, *Sci. Rep.* **2018**, *8*, 14518.
[143] B. Liu, F. Chen, S. Wang, Z. Fu, T. Cheng, T. Li, *J. Appl. Mech.* **2017**, *84*, 091005.
[144] T. Y. Cheng, G. R. Li, Y. M. Liang, M. Q. Zhang, B. Y. Liu, T. W. Wong, J. Forman, M. H. Chen, G. Y. Wang, Y. Tao, T. F. Li, *Smart Mater. Struct.* **2019**, *28*, 015019.
[145] J. Shintake, H. Shea, D. Floreano, in *2016 IEEE/RSJ Int. Conf. on Intelligent Robots and Systems (IROS)*, Daejeon, Korea **2016**, p. 4957.
[146] F. Berlinger, M. Duduta, H. Gloria, D. Clarke, R. Nagpal, R. Wood, in *2018 IEEE Int. Conf. on Robotics and Automation (ICRA)*, Brisbane, Australia **2018**, p. 3429.
[147] Y. C. Tang, L. Qin, X. N. Li, C. M. Chew, J. Zhu, in *IEEE Int. Conf. on Intelligent Robots*, Vancouver, BC, Canada **2017**, p. 2403.
[148] T. Li, G. Li, Y. Liang, T. Cheng, J. Dai, X. Yang, B. Liu, Z. Zeng, Z. Huang, Y. Luo, T. Xie, W. Yang, *Sci. Adv.* **2017**, *3*, e1602045.
[149] G. Li, X. Chen, F. Zhou, Y. Liang, Y. Xiao, X. Cao, Z. Zhang, M. Zhang, B. Wu, S. Yin, Y. Xu, H. Fan, Z. Chen, W. Song, W. Yang, B. Pan, J. Hou, W. Zou, S. He, X. Yang, G. Mao, Z. Jia, H. Zhou, T. Li, S. Qu, Z. Xu, Z. Huang, Y. Luo, T. Xie, J. Gu, et al., *Nature* **2021**, *591*, 66.
[150] C. Christianson, N. N. Goldberg, D. D. Deheyn, S. Cai, M. T. Tolley, *Sci. Robot.* **2018**, *17*, eaat1893.
[151] G. Kovacs, P. Lochmatter, M. Wissler, *Smart Mater. Struct.* **2007**, *16*, S306.
[152] T. Lu, Z. Shi, Q. Shi, T. J. Wang, *Extreme Mech. Lett.* **2016**, *6*, 75.
[153] U. Gupta, Y. Wang, H. Ren, J. Zhu, *IEEE-ASME Trans. Mechatron.* **2019**, *24*, 25.
[154] Y. Wang, J. Zhu, *Extreme Mech. Lett.* **2016**, *6*, 88.
[155] F. Carpi, D. De Rossi, *Bioinspir. Biomim.* **2007**, *2*, S50.
[156] Y. Liu, L. Shi, L. Liu, Z. Zhang, J. Leng, in *Electroactive Polymer Actuators and Devices (EAPAD) 2008*, Vol. *69271*, San Diego, CA **2008**, p. 69271A.
[157] L. Li, H. Godaba, H. Ren, J. Zhu, *IEEE-ASME Trans. Mechatron.* **2019**, *24*, 100.
[158] F. Carpi, G. Frediani, S. Turco, D. De Rossi, *Adv. Funct. Mater.* **2011**, *21*, 4152.
[159] M. Ghilardi, H. Boys, P. Torok, J. J. C. Busfield, F. Carpi, *Sci. Rep.* **2019**, *9*, 16127.
[160] S. Shian, R. M. Diebold, D. R. Clarke, *Opt. Express* **2013**, *21*, 8669.
[161] J. R. Li, Y. Wang, L. W. Liu, S. Xu, Y. J. Liu, J. S. Leng, S. Q. Cai, *Adv. Funct. Mater.* **2019**, *29*, 1903762.
[162] I. Koo, K. Jung, J. Koo, J. D. Nam, Y. Lee, H. R. Choi, in *2006 SICE-ICASE Int. Joint Conf.*, Bexco, Busan **2006**, p. 4823.
[163] H. S. Lee, H. Phung, D.-H. Lee, U. K. Kim, C. T. Nguyen, H. Moon, J. C. Koo, J.-d. Nam, H. R. Choi, *Sens. Actuators, A* **2014**, *205*, 191.
[164] M. Matysek, P. Lotz, T. Winterstein, H. F. Schlaak, in *Third Joint Eurohaptics Conf. and Symp. on Haptic Interfaces for Virtual Environment and Teleoperator Systems*, IEEE, Piscataway, NJ **2009**, p. 290.
[165] L. E. Knoop, J. Rossiter, in *Electroactive Polymer Actuators and Devices (EAPAD) 2014*, Vol. *9056*, San Diego, CA **2014**, p. 905610.
[166] A. Marette, A. Poulin, N. Besse, S. Rosset, D. Briand, H. Shea, *Adv. Mater.* **2017**, *29*, 1700880
[167] S. Yun, S. Park, B. Park, S. Ryu, S. M. Jeong, K.-U. Kyung, *IEEE Trans. Ind. Electron.* **2020**, *67*, 717.
[168] X. Ji, X. Liu, V. Cacucciolo, Y. Civet, A. El Haitami, S. Cantin, Y. Perriard, H. Shea, *Adv. Funct. Mater.* **2020**, https://doi.org/10.1002/adfm.202006639.
[169] H. Zhao, A. M. Hussain, A. Israr, D. M. Vogt, M. Duduta, D. R. Clarke, R. J. Wood, *Soft Robot.* **2020**, *7*, 451.
[170] A. Poulin, S. Rosset, H. R. Shea, *Appl. Phys. Lett.* **2015**, *107*, 244104.
[171] S. Rosset, C. de Saint-Aubin, A. Poulin, H. R. Shea, *Rev. Sci. Instrum.* **2017**, *88*, 105002.
[172] C. A. de Saint-Aubin, S. Rosset, S. Schlatter, H. Shea, *Smart Mater. Struct.* **2018**, *27*, 074002.
[173] J. W. Cao, W. Y. Liang, Q. Y. Ren, U. Gupta, F. F. Chen, J. Zhu, in *2018 IEEE Int. Conf. on Robotics and Automation (ICRA)*, Brisbane, Australia **2018**, p. 4188.
[174] C. Huu Nguyen, G. Alici, R. Mutlu, *J. Mech. Des.* **2014**, *136*, 061009.
[175] G. Rizzello, D. Naso, A. York, S. Seelecke, *IEEE Trans. Control Syst. Technol.* **2015**, *23*, 632.
[176] N. H. Chuc, N. H. L. Vuong, D. S. Kim, H. P. Moon, J. C. Koo, Y. K. Lee, J.-D. Nam, H. R. Choi, *IEEE-ASME Trans. Mechatron.* **2011**, *16*, 167.
[177] B. O'Brien, J. Thode, I. Anderson, E. Calius, E. Haemmerle, S. Xie, in *Electroactive Polymer Actuators and Devices (EAPAD) 2007*, Vol. *6524*, San Diego, CA **2007**, p. 652415.
[178] G. Mao, L. Wu, Y. Fu, Z. Chen, S. Natani, Z. Gou, X. Ruan, S. Qu, *IEEE-ASME Trans. Mechatron.* **2018**, *23*, 2132.
[179] J. J. Loverich, I. Kanno, H. Kotera, *Lab Chip* **2006**, *6*, 1147.
[180] Y. Guo, L. Liu, Y. Liu, J. Leng, *Extreme Mech. Lett.* **2021**, *42*, 101134.
[181] R. Sarban, R. W. Jones, B. R. Mace, E. Rustighi, *Mech. Syst. Signal Proc.* **2011**, *25*, 2879.
[182] R. Heydt, R. Kornbluh, J. Eckerle, R. Pelrine, in *Smart Structures and Materials 2006: Electroactive Polymer Actuators and Devices (EAPAD)*, Vol. *6168*, San Diego, CA **2006**, p. 61681M.
[183] N. Hosoya, S. Baba, S. Maeda, *J. Acoust. Soc. Am.* **2015**, *138*, EL424.
[184] A. Poulin, M. Imboden, F. Sorba, S. Grazioli, C. Martin-Olmos, S. Rosset, H. Shea, *Sci. Rep.* **2018**, *8*, 9895.
[185] M. Imboden, E. de Coulon, A. Poulin, C. Dellenbach, S. Rosset, H. Shea, S. Rohr, *Nat. Commun.* **2019**, *10*, 834.
[186] Y. Bar-Cohen, S. Rosset, H. R. Shea, A. Poulin, in *Electroactive Polymer Actuators and Devices (EAPAD) XX*, Vol. *10594*, SPIE, Denver, CO **2018**, p. 105940V.
[187] Y. Li, J. Li, L. Liu, Y. Yan, Q. Zhang, N. Zhang, L. He, Y. Liu, X. Zhang, D. Tian, J. Leng, L. Jiang, *Adv. Sci.* **2020**, *7*, 2000772.
[188] X. F. Lv, L. W. Liu, Y. J. Liu, J. S. Leng, *Smart Mater. Struct.* **2015**, *24*, 115036.
[189] G. Moretti, G. P. Rosati Papini, L. Daniele, D. Forehand, D. Ingram, R. Vertechy, M. Fontana, *Proc. Math. Phys. Eng. Sci.* **2019**, *475*, 20180566.
[190] J. Liu, G. Mao, X. Huang, Z. Zou, S. Qu, *J. Appl. Mech.* **2015**, *82*, 101004.
[191] J. Kim, J. W. Kim, H. C. Kim, L. Zhai, H.-U. Ko, R. M. Muthoka, *Int. J. Precision Eng. Manuf.* **2019**, *20*, 2221.
[192] J.-H. Youn, S. M. Jeong, G. Hwang, H. Kim, K. Hyeon, J. Park, K.-U. Kyung, *Appl. Sci.* **2020**, *10*, 640.
[193] R. D. Kornbluh, R. Pelrine, Q. Pei, S. Oh, J. Joseph, in *Smart Structures and Materials 2000: Electroactive Polymer Actuators and Devices (EAPAD)*, Vol. *3987*, Newport Beach, CA **2000**, p. 51.
[194] S. I. Rich, R. J. Wood, C. Majidi, *Nat. Electron.* **2018**, *1*, 102.
[195] S. M. Mirvakili, I. W. Hunter, *Adv. Mater.* **2018**, *30*, 1704407.
[196] K. B. Subramani, R. J. Spontak, T. K. Ghosh, *Compos. Sci. Technol.* **2018**, *154*, 187.

[197] C. Xu, G. T. Stiubianu, A. A. Gorodetsky, *Science* **2018**, *359*, 1495.
[198] W.-B. Li, W.-M. Zhang, H.-X. Zou, Z.-K. Peng, G. Meng, *Smart Mater. Struct.* **2016**, *25*, 115023.
[199] H. Godaba, C. C. Foo, Z. Q. Zhang, B. C. Khoo, J. Zhu, in *Electroactive Polymer Actuators and Devices (EAPAD) 2015*, Vol. *9430*, San Diego, CA **2015**, p. 94302C.
[200] L. Hines, K. Petersen, M. Sitti, *Adv. Mater.* **2016**, *28*, 3690.
[201] L. Chen, W. Chen, Y. Xue, M. Zhang, X. Chen, X. Cao, Z. Zhang, G. Li, T. Li, *J. Appl. Mech.* **2019**, *86*, 031004.
[202] C. Cao, S. Burgess, A. T. Conn, *Front. Robot. AI* **2018**, *5*, 137.
[203] M. Adachi, K. Hamazawa, Y. Mimuro, H. Kawamoto, *J. Electrost.* **2017**, *89*, 88.
[204] E. Hajiesmaili, E. Khare, A. Chortos, J. Lewis, D. R. Clarke, *Extreme Mech. Lett.* **2019**, *30*, 100504.
[205] C. T. Nguyen, H. Phung, P. T. Hoang, T. D. Nguyen, H. Jung, H. Moon, J. C. Koo, H. R. Choi, in *IEEE Int. Conf. on Intelligent Robots*, IEEE, Piscataway, NJ **2017**, p. 6233.
[206] M. Duduta, D. R. Clarke, R. J. Wood, in *IEEE Int. Conf. on Robotics and Automation (ICRA)*, SPIE, Piscataway, NJ **2017**, p. 4346.
[207] S. Shian, K. Bertoldi, D. R. Clarke, in *Electroactive Polymer Actuators and Devices (Eapad) 2015*, Vol. *9430*, San Diego, CA **2015**.
[208] L. Xu, H. Q. Chen, J. Zou, W. T. Dong, G. Y. Gu, L. M. Zhu, X. Y. Zhu, *Bioinspir. Biomim.* **2017**, *12*, 025003.
[209] J. Shintake, V. Cacucciolo, H. Shea, D. Floreano, *Soft Robot.* **2018**, *5*, 466.
[210] C. Tang, W. Ma, B. Li, M. Jin, H. Chen, *Adv. Eng. Mater.* **2019**, *22*, 1901130.

Yaguang Guo received his B.S. in engineering mechanics in 2017 from Northeast Petroleum University. He is currently a Ph.D. candidate under the supervision of Professor Liwu Liu at Harbin Institute of Technology. His research interests focus on dielectric elastomer actuators and soft robotics.

Liwu Liu is a full professor in the Department of Aerospace Science and Mechanics at the Harbin Institute of Technology (HIT), China. He received his Ph.D. in solid mechanics from HIT in 2012. His research interests include electroactive polymers, soft robotics, shape memory polymers, and their composites.

Yanju Liu is a full professor in the Department of Aerospace Science and Mechanics at the Harbin Institute of Technology (HIT), China. She obtained her Ph.D. in material science from HIT, China in 1999. Her research interests are in the field of smart materials and structures, including stimuli–responsive materials, such as electrorheological/magnetorheological fluids, electroactive polymers, shape memory polymers, and their composites.

Jinsong Leng is a Cheung Kong Chair Professor at Harbin Institute of Technology (HIT). He received his B.S. and Ph.D. in engineering mechanics and composite materials from HIT in 1990 and 1996, respectively. He is the director of the Center for Smart Materials and Structures (http://smart.hit.edu.cn/). His research interests cover shape memory polymers and composites, 4D printing, sensors and actuators, structural health monitoring, and multifunctional nanocomposites.